2016

# Chemical Characterization and Source Apportionment of Ambient PM2.5 over Key Emission Regions in China

Zhou, Jiabin

UNIVERSITY OF CALGARY

# Chemical Characterization and Source Apportionment of Ambient $PM_{2.5}$ over Key Emission Regions in China

by

Jiabin Zhou

A THESIS

SUBMITTED TO THE FACULTY OF GRADUATE STUDIES

IN PARTIAL FULFILMENT OF THE REQUIREMENTS FOR THE

DEGREE OF MASTER OF SCIENCE

GRADUATE PROGRAM IN MECHANICAL AND MANUFACTURING ENGINEERING

CALGARY, ALBERTA

AUGUST, 2016

## Abstract

A year-round campaign was completed for comprehensive characterization of $PM_{2.5}$ over four key emission regions in China. The annual average $PM_{2.5}$ mass concentrations ranged from 60.5 to 148.9 μg $m^{-3}$. Nine water-soluble ions collectively contributed 33–41% of $PM_{2.5}$ mass, with three dominant ionic species being $SO_4^{2-}$, $NO_3^-$, $NH_4^+$, and carbonaceous particulate matter contributed 16-23% of the $PM_{2.5}$ mass. The characteristic chemical species combined with back trajectory analysis indicated that Wuqing site was heavily influenced by air masses originating from Mongolia and North China Plain regions, whereas Deyang site suffered from both local emissions of Sichuan Basin and biomass burning via long-range transport from South Asia. A molecular marker-chemical mass balance (MM-CMB) receptor model revealed that the major primary contributors to $PM_{2.5}$ OC were vehicle emission, coal combustion, biomass burning, meat cooking and natural gas combustion, which collectively accounted for 84±24% of measured OC. The major contributors to $PM_{2.5}$ mass were secondary sulfate (26-30%), vehicle emission (12-26%), secondary nitrate (12-23%), coal combustion (6-12%), secondary ammonium (7-9%), biomass burning (4-12%), meat cooking (2-5%), natural gas combustion (1-2%), and other OM (2-13%) on annual average at these sites. This study found the source apportionment has distinct regional and seasonal characteristics. This knowledge is essential for government to make region specific control strategies for fine particles pollution in China.



***Keywords***: $PM_{2.5}$; air quality; source apportionment; carbonaceous aerosol; China

**Acknowledgements**

First and foremost I would like to thank my supervisor, Professor Ke Du, for his encouragement, support, and guidance throughout my graduate study. His diligence, preciseness, and creativity significantly influenced and raised me up to the next level in the field of atmospheric pollution.

I would also like to thank my MS committee members (Profs. Craig Johansen, Seonghwan Kim, and Hua Song) for their comments and helps on my thesis.

I thank NSERC Discovery Grant, Queen Elizabeth II Scholarships, and the Strategic Priority Research Program (B) of the Chinese Academy of Sciences (XDB05060200) for financial support of this research. I thank the Department of Mechanical and Manufacturing Engineering and the University of Calgary for the facilities support of my work. I am grateful for the help from all faculties, staffs, and students in the Department of Mechanical and Manufacturing Engineering and the Faculty of Graduate Studies (FGS).

I would like to express my gratitude to the following individuals in Prof. Du's group for their unselfish help and contributions: Kuangyou Yu, Xiaoyan Huang, Zhenyu Xing. I thank Zhenyu Xing and Junjun Deng for their assistance with sample collect and analysis.

Finally, I would like to thank my family for their love and support during my graduate study.

## Dedication

This work is dedicated to my family members who have sacrificed so much to support me study at the University of Calgary.

## Table of Contents

## List of Tables

## List of Figures and Illustrations

## List of Symbols, Abbreviations, and Nomenclature

| Symbol | Definition |
|---|---|
| OC | Organic carbon |
| OM | Organic matter |
| TC | Total carbon |
| EC | Element carbon |
| BC | Black carbon |
| HMW | High molecular weight |
| PAHs | Polycyclic aromatic hydrocarbons |
| PM | Particulate matter |
| POA | Primary organic aerosols |
| SOA | Secondary organic aerosol |
| SOC | Secondary organic carbon |
| VOCs | Volatile organic compounds |
| WSOC | Water-soluble organic carbon |
| CCN | Cloud condensation nuclei |
| PCA | Principal component analysis |
| CMB | Chemical mass balance |
| PMF | Positive matrix factorization |
| RSD | Relative standard deviation |
| NAAQS | National Ambient Air Quality Standards |
| BTH | Beijing-Tianjin-Hebei |
| NCP | North China Plain |
| YRD | Yangzi River Delta |
| PRD | Pearl River Delta |
| SB | Sichuan Basin |
| $b_{ext}$ | light extinction coefficient |

# Chapter 1: Introduction

## 1.1 Background and motivation

Atmospheric aerosols have significant impacts on global climate, human health, and visibility reduction. Aerosol particulate matter (PM) in the lower atmosphere is composed of water soluble inorganic salts, insoluble mineral dust, and carbonaceous material. Numerous epidemiological studies indicated that elevated concentration of fine particulate matter in the atmosphere is associated with adverse effects on the respiratory and cardiovascular systems (Harrison and Yin, 2000; Pope and Dockery, 2006).

The impairment of visibility is attributed primarily to the scattering and absorption of visible light by suspended particles, and gaseous pollutants, as well as meteorological conditions. Among them, the aerosol fine particulate matter is believed to be mostly responsible for the scattering of visible light and to cause the degradation of visibility. PM is a mixture of physical and chemical characteristics varying by location. On a global scale, the distribution of fine PM in the atmosphere is highly non-homogeneous. According to the WHO, there is mounting evidence that concentration of PM is increasing in Asia. In many cities the levels of fine PM are exceeding the critical limit, specifically in densely populated, fast-growing and less developed countries like India, China, Pakistan. Nowadays, most of the megacities in China suffered haze pollution with a high level of $PM_{2.5}$ pollutants (PM with an aerodynamic diameter of 2.5 μm or less) due to fast industrialization and urbanization in the past decades. Ambient $PM_{2.5}$ has become as the primary pollutant since most of the Chinese cities cannot meet the new National Ambient Air Quality Standards (NAAQS) of China for $PM_{2.5}$ (Annual mean: 35 μg $m^{-3}$; 24-hour mean: 75 μg $m^{-3}$). Previous studies revealed that Beijing-Tianjin-Hebei area (BTH), Yangtze River Delta area

(YRD), Pearl River Delta area (PRD) and Sichuan Basin area (SB) are the four major black carbon (BC) emission areas in China (Cao et al., 2006; Xing et al., 2014).

Atmospheric aerosols are formed from a wide variety of natural and anthropogenic sources. Particulate matter may be either directly emitted from the primary sources or formed from gas precursors undergo chemical reactions and physical transformations. Aerosol particulate matter consists of a host of chemical species including carbonaceous components, trace metals, sulfate, nitrate, ammonium, and many others. It is important to understand what make up the aerosol and how the chemical composition of the aerosol is temporally and spatially distributed in the ambient environment. Source apportionment method is a valuable tool to estimate emissions contributions to particulate matter thereby the effective control strategies can be developed. The chemical compositions of atmospheric PM, especially molecular marker, are the primary input data that can be used to get reliable model results (Paode et al., 1999). Due to the complex nature of air pollution as well as the limitations of each individual source apportionment approach, there is considerable uncertainty in the estimation of source contributions. Therefore, there is a great need to validate these models so as to establish consistency between model predictions and ambient observations.

### 1.2 Research objectives

The main objectives of this study are to

(1) Investigate the detailed chemical composition of $PM_{2.5}$ over four key emission regions in China.

(2) Study the effect of regional transport on the seasonal variation of $PM_{2.5}$ across the sites.

(3) Estimate the source contributions to organic carbon (OC) and $PM_{2.5}$ mass using receptor model.

### 1.3 Thesis overview

Besides this chapter, five chapters are remaining in this thesis. Chapter 2 provides literature reviews on aerosol PM sizes and chemical characterization, climate and health effects of PM, chemical transformation and regional transport, and source apportionment of PM. Chapter 3 provides sampling sites information and experimental method including sampling and chemical analysis, air masses back trajectories analysis, CMB receptor model. Chapter 4 focuses on water soluble ions observed over the four sites in China, and their potential sources and transport processes are also discussed in detail. Chapter 5 discusses organic composition and source apportionment of $PM_{2.5}$ using molecular marker based CMB model. Finally, conclusions along with future research expectation are summarized in Chapter 6.

During the study, my group members collected $PM_{2.5}$ samples and conducted measurement of water soluble ions, EC and OC. I made PCA analysis to identify the major sources for water soluble ions. I extracted organic fractions from aerosol samples and quantified individual organic compounds using GC-MS. Meanwhile, I investigated the transport of air mass using HYSPLIT model, and set up the MM-CMB model to estimate the primary source contributions to OC and $PM_{2.5}$ mass.

# Chapter 2: Literature Review

## 2.1 PM sizes and chemical composition

Atmospheric PM is ubiquitous in the earth's atmosphere and consists of a heterogeneous mixture of small particles and liquid droplets varying greatly in size, composition, and origin (WHO, 2013; Kim et al., 2015). Atmospheric PM is of considerable concern because it has pronounced effect on global climate, human health, and visibility reduction.

Atmospheric aerosol particles range in size over a few orders of magnitude. PM is commonly defined by three general categories (U.S. EPA): coarse (2.5 to 10 μm), fine (2.5 μm or smaller), and ultrafine (0.1 μm or smaller). Figure 2-1 illustrates a current understanding of ambient particle size distributions with multiple modes. The size of particles is directly linked to their potential for causing health problems since it influences how particles deposit in the respiratory tract. The health effects of PM mainly depend on particle size, the amount of inhaled particles, and the exposure time. Fine particles are more likely to causes adverse health effects than coarse particles because it will more deeply penetrate into the lungs and blood streams. Meanwhile, fine and ultrafine particles have greater surface area than larger particles of the same mass, and they are likely to adsorb more toxic species.

The PM in the atmosphere is generally composed of a broad range of chemical species, including water-soluble ions (e.g., sulfate, nitrate, ammonium), metals (iron, magnesium, copper, nickel, vanadium, zinc), crustal material, carbonaceous components (elemental carbon, alkanes, polycyclic aromatic hydrocarbons), and biological components (allergens and microbial) (Seinfeld and Pandis, 2006; Cheung et al., 2011).

In general, water-soluble ions commonly account for one-third of particulate matter mass in the

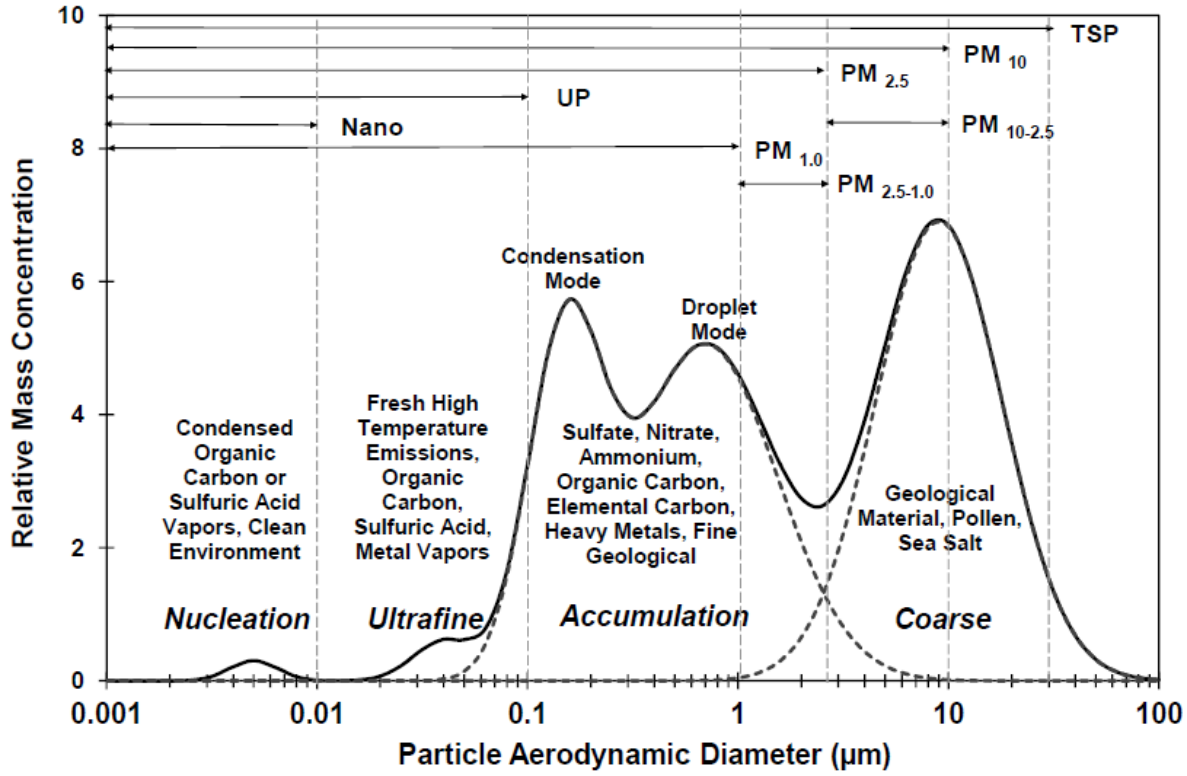


Figure 2-1 Idealized example of an ambient particle size distribution, patterned after Chow (1995) and Watson (2002), adapted from Cao (2013).

urban atmosphere, among which the main constituents are the secondary particulate compounds such as sulfate, nitrate, and ammonium. Particulate sulfate in atmospheric aerosols could account for up to approximately 40% of all water-soluble species (Kiss et al., 2000). Sulfate is directly emitted or generated by oxidation of sulfur dioxide ($SO_2$), dimethyl sulfide and hydrogen sulfide (Brimblecombe, 1996). Particulate nitrate arises primarily from the oxidation of $NO_x$ (Yang et al., 2004). Numerous studies indicated that sulfate and ammonium mainly existed in the fine particles, while the nitrate can be found in both the coarse and fine modes (Lestaria et al., 2003; Zhao and Gao, 2008).

The organic aerosol is a significant constituent of aerosol particles mass, contributing 20–50% of the total fine aerosol mass at continental mid-latitudes (Saxena and Hildemann., 1996) and as high as 70% in tropical forested areas (Roberts et al., 2001). The atmospheric carbonaceous aerosol is classified as elemental carbon, organic material, and carbonate minerals. The organic material consists of thousands of compounds with very different physical and chemical properties.

A considerable effort has been undertaken to characterize the chemical composition of atmospheric aerosols. Currently, hundreds of non-polar organic compounds have been characterized in airborne PM. However, little is known about polar and water-soluble organic compounds (WSOC), which account for 20 to 70% of the total organic carbon (Saxena and Hildemann, 1996; Kiss et al., 2000). Even in the most comprehensive investigations, only 10–40% of the organic aerosol particles content estimated from OC measurements has been unambiguously identified on a molecular level (Schauer et al., 2002).

**2.2 Climate and health effect**

Atmospheric aerosols influence the earth's radiative balance in many ways. Aerosol effects on climate are classified as direct or indirect with respect to radiative forcing of the climate system.

The direct aerosol effect consists of any direct interaction of radiation with atmospheric aerosols, such as absorption or scattering. It affects both short and longwave radiation to produce a net negative radiative forcing. The magnitude of the resultant radiative forcing due to the direct effect of an aerosol is dependent on the albedo of the underlying surface, as this affects the net amount of radiation absorbed or scattered to space.

The indirect aerosol effect consists of any change to the earth's radiative budget due to the modification of clouds by atmospheric aerosols. Cloud droplets form onto pre-existing aerosol particles, known as cloud condensation nuclei (CCN). For any given meteorological conditions, an increasing amount of CCN leads to an increase in the number of cloud droplets. This could cause more scattering of shortwave radiation i.e. an increase in the albedo of the cloud, known as the cloud albedo effect (Seinfeld and Pandis, 2006).

Numerous epidemiological studies have shown that PM is responsible for a wide range of health consequences such as cardiovascular and respiratory diseases (Pope and Dockery, 2006; Schulz et al., 2005). More than two million deaths occur globally each year is caused by exposure to fine particulate matter (Shah et al., 2013).

In general, the airborne particulate matter is rarely homogeneous, and it may vary greatly in size, shape, and chemical composition. The size of the particle is a main determinant of where in the respiratory tract the particle will come to rest when inhaled. Because of their small size, particles on the order of ~10 micrometers or less ($PM_{10}$) can penetrate the deepest part of the lungs such as the bronchioles or alveoli. Larger particles are generally filtered in the nose and throat. The particles smaller than 2.5 micrometers, $PM_{2.5}$, tend to penetrate into the gas-exchange regions of the lung, and very small particles (< 100 nanometers) may pass through the lungs to affect other organs. The European Study of Cohorts for Air Pollution Effects (ESCAPE) reported that an increase in estimated annual exposure to $PM_{2.5}$ of 5 $\mu g\ m^{-3}$ was linked with a 13% increased risk of heart attacks (Pope et al., 2002; Mohapatra and Biswal, 2014). Researchers suggest that even short-term exposure to elevated concentrations could significantly contribute to heart disease. The health effect of particles is not wholly dependent on their size, while the chemical constitute

plays a part. Particles emitted from modern diesel engines are typically in the size range of 100 nanometers, and these soot particles can carry carcinogenic components like benzo(a)pyrene adsorbed on their surface. It may be even more damaging to the cardiovascular system.

Scientific studies provide ample evidence of the relationship between exposure to short-term and long-term ambient particulate concentrations and human mortality and morbidity effects. To date, however, the dose-response mechanism is not yet fully understood. Furthermore, according to WHO (2013), there is no safe threshold level below which health damage does not occur.

### 2.3 Light extinction and visibility

Visibility conditions are commonly expressed in terms of visual range and light extinction. Visual range is the maximum distance at which one can identify a black object against the horizon. Light extinction, inversely related to visual range, is the sum of light scattering and light absorption by particles and gases in the atmosphere. Visibility impairment has become an important environmental issue receiving close attention from both the scientific community and the public.

Early in 1987, the IMPROVE visibility monitoring network was established in U.S. It aims to provide information for determining the types of pollutants and sources primarily responsible for visibility impairment. Chemical analysis of aerosol measurements at more than 70 Class I sites provided ambient concentrations and associated light extinction for $PM_{10}$, $PM_{2.5}$, sulfates, nitrates, organic and elemental carbon, soil dust, and a number of other elements. In Eastern U.S., the reduced visibility is mainly attributed to secondary particulate matter, whereas the primary emissions from the sources such as wood smoke reduce visibility at a higher percentage in

Western U.S. (IMPROVE, 2000). Numerous studies have indicated that the impairment of visibility is attributed primarily to the scattering and absorption of visible light by suspended particles, and gaseous pollutants, as well as meteorological conditions. Among them, aerosol fine PM has a size close to wavelengths in the visible range and thus is believed to be mostly responsible for the scattering of visible light and to cause the degradation of visibility.

Previous studies have demonstrated that the size, chemical composition, and concentration of airborne particles heavily influence visibility. Although natural emissions can be involved, emissions of anthropogenic pollutants are the primary cause for degrading atmospheric visibility. Xiao et al. (2014) investigated the trend in visibility change from 1980 to 2012 in Baoji, China based on long-term meteorological data and field measurement on PM compositions, and revealed that $PM_{2.5}$ organic matter (OM) contributes to 34.2% of the light extinction coefficient ($b_{ext}$) on an annual basis (Figure 2-2), followed by $(NH_4)_2SO_4$ (30.0%), $NH_4NO_3$ (20.1%), elemental carbon (9.2%) and soil dust (6.5%). Tiwari et al. (2014) analyzed the mass of $PM_{2.5}$ particles, BC, NOx, extinction coefficient ($b_{ext}$), and meteorological parameters over Delhi, India during the winter period. It was found that the largest contribution in the light extinction coefficients was organic carbon (46%), followed by elemental carbon (24%), coarse mode particles (18%), ammonium sulfate (8%) and ammonium nitrate (4%).

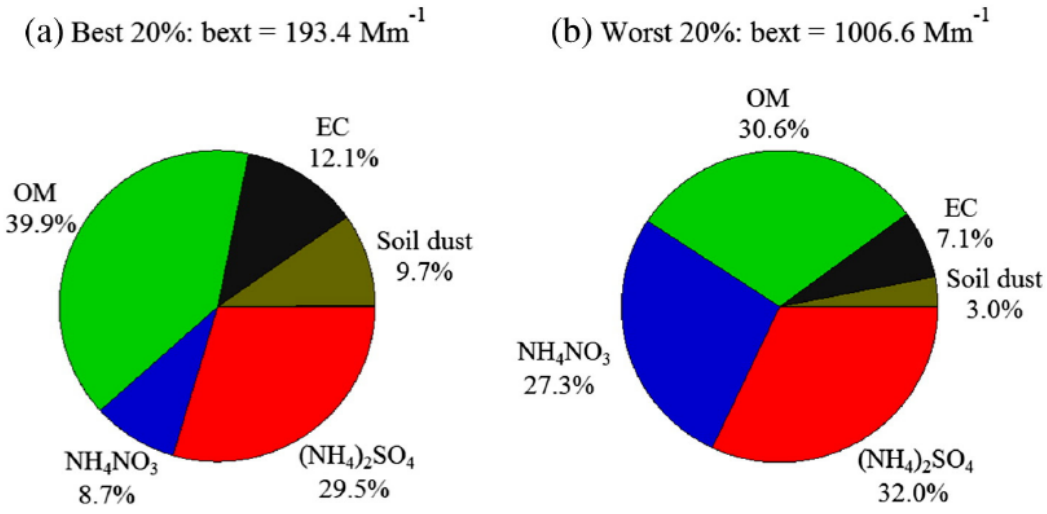


Figure 2-2 Relative source contributions to chemical light extinction for the best 20% and the worst 20% of the annual visual range in Baoji between 2012 and 2013

### 2.4 Chemical transformation and regional transport

Airborne PM may be either directly emitted into the atmosphere (primary sources) or formed by gas-particle conversion (secondary sources). Atmospheric aerosol transformations and gas-particle interactions generally involve multiple physicochemical processes such as mass transport, phase transition, nucleation, condensation, heterogeneous and multiphase chemical reactions. The relative contributions of these two source processes depend on the local types of emissions, meteorology and atmospheric chemical conditions in the area.

The formation of aerosol sulfate from $SO_2$ is usually by means of homogeneous gas phase reaction of $SO_2$ with OH radical, heterogeneous reactions in the aqueous surface layer of pre-existing particles, and in-cloud processes (Meng and Seinfeld, 1994). Du et al. (2011) investigated the water-soluble ionic composition of aerosols over Shanghai during summertime

haze pollution events and revealed that substantial amount of precursor gases of $SO_2$ and $NO_2$ were oxidized into $SO_4^{2-}$ and $NO_3^-$ on the surface of pre-existing KCl particles under high atmospheric oxidation ability and steady atmosphere condition.

Gaseous $HNO_3$ and $N_2O_5$ are major precursors of aerosol nitrate. $HNO_3$ is predominantly formed by homogeneous gas phase reactions of $NO_2$ with OH radical and heterogeneous chemistry involving the hydrolysis of $N_2O_5$ on aerosol surfaces (Pathak et al., 2009).

Organic aerosol components can be classified as primary or secondary. Both primary and secondary aerosols can be of either anthropogenic or natural origin. Primary organic aerosol (POA) components are directly emitted in the condensed phase (liquid or solid particles) or as semi-volatile vapors, which are condensable under atmospheric conditions.

Most of the information on sources of secondary organics comes from controlled laboratory smog chamber experiments where gases that have been measured in the atmosphere are introduced into a chamber and allowed to react with an oxidant. Secondary organic aerosol (SOA) is commonly produced by ozone or radical-initiated reactions of hydrocarbon precursors, producing nonvolatile and semi-volatile organic products which can undergo nucleation reactions to form new particles or condense onto pre-existing particulate matter (Seinfeld et al., 2001).

The major classes of SOA precursors are volatile and semi-volatile alkanes, alkenes, aromatic hydrocarbons, and oxygenated compounds. Anthropogenic emissions consist of ~40% alkanes, ~10% alkenes, and ~20% aromatics, with the rest being oxygenated and unidentified compounds. Biogenic emissions are mostly alkenes, being ~50% isoprene and ~10% monoterpenes, with the rest being other reactive and unidentified VOC (some of which are also alkenes, such as

sesquiterpenes). Biogenic emissions contribute ~90% of non-methane VOCs globally, with anthropogenic emissions being more important in urban areas (Robinson et al., 2007).

Secondary organic aerosol (SOA) components are formed through the chemical reaction of biogenic and anthropogenic gaseous precursors in the atmosphere, which may proceed through different pathways. It is possibly formed by new particle formation, gas-particle partitioning, heterogeneous or multiphase reactions (Seinfeld et al., 2001). The actual atmospheric SOA formation pathways and involved chemical reaction mechanisms, however, still remain to be clarified.

In the atmosphere, coarse and fine particles behave in different ways. Coarse particles may settle out from the air more rapidly than fine particles and will be found close to their emission sources. Fine particles, however, is easily subject to long-range transport by wind and can travel thousands of miles from the source of origin.

Findings from previous studies indicate that anthropogenic air pollutants from European sources can be transported over long distances, reaching Africa, the Atlantic Ocean, and North America. The PM of natural origin, like Saharan dust, can be transported toward the Atlantic Ocean and North America mostly during the warm period of the year (Kallos et al., 2007). Both local and regional sources contribute to particle pollution. It was found that in the eastern half of the U.S., regional anthropogenic emissions, natural aerosols, and long-range transport of anthropogenic aerosols from other regions contribute about 62%, 32%, and 6% to surface $PM_{2.5}$, respectively, while in the western U.S. the percentages are 28%, 60%, and 12% base on the global model GOCART (Chin et al., 2002).

## 2.5 Source apportionment of PM

Source apportionment is the process of apportioning ambient air pollutants at a receptor site to their respective sources. Source apportionment is a valuable scientific and regulatory tool to quantitatively understand the impact of individual source emission on air pollutants. In principle, source apportionment can be performed in complementary ways. The traditional approach is dispersion model, which implements mathematical simulation of how air pollutants disperse in the atmosphere. It is performed with pollutant emission rate and meteorological data, generating a prediction of resulting downwind ambient concentration of pollutants. The alternative is receptor model, which is defined as "a specified mathematical procedure for identifying and quantifying the sources of ambient air contaminants at a receptor primarily on the basis of concentration measurements at that receptor" (Chow et al., 2006).

Receptor models are mathematical or statistical procedures for identifying and quantifying the sources of air pollutants at a receptor location. The key outputs are the percentage contributions of different sources to pollutant concentration. Such models are particularly helpful in cases where complete emissions inventories are not available (Hopke, 1991). Unlike dispersion air quality models, receptor models do not use pollutant emissions, meteorological data, and chemical transformation mechanisms to estimate the contribution of sources to receptor concentrations. Instead, receptor models use the chemical and physical characteristics of gases and particles measured at source and receptor to both identify the presence of and to quantify source contributions to receptor concentrations. These models are therefore a natural complement to other air quality models.

Source apportionment for primary aerosol is relatively simple to obtain because source-receptor

relationships are essentially linear for primary pollutants. The dispersion models, such as Gaussian steady-state models and Lagrangian puff models, have been used extensively to model primary aerosol pollution from specific sources (Dunker et al., 2002; Kleeman and Cass, 2001). The Gaussian and Lagrangian approaches work for primary aerosol because the models assume that emissions from separate sources do not interact. This assumption, however, breaks down for secondary aerosol pollutants (e.g., sulfate, nitrate, ammonium, SOA).

Receptor modeling techniques are based on the evaluation of data acquired at receptor sites, and most of them do not require previously identified emission sources. Examples of receptor models are Chemical Mass Balance (CMB), Positive Matrix Factorization (PMF) and Principal Component Analysis (PCA). CMB fully apportions receptor concentrations to chemically distinct source-types depending upon a source profile database, while PMF does not require any information as input to the model and generate source profiles and contributions from the ambient data.

Since PM is composed of both inorganic (trace metals, cations, and anions) and organic species, a range of source markers are used in receptor modeling studies. Traditionally, most studies were carried out using inorganic trace elements such as Fe, Zn, Pb, Ca, Mg, and Al. However, since many of the trace elements are emitted from a range of sources (e.g., Zn is emitted from tyre wear as well as refuse burning), it was difficult to apportion the PM to sources with a high degree of confidence. Additionally, with the removal of some elements (i.e. Pb) from gasoline, there has been a need to develop new source markers. In the last two decades, research has focused on developing organic molecular markers that can be characteristic of sources. These molecular markers once applied to receptor model, and it could greatly reduce the source ambiguity

(Simoneit et al., 1999; Schauer et al., 1996; Robinson et al., 2006). Receptor-based models have been used in the past to understand sources of elemental carbon and organic carbon (EC, OC), which comprise carbonaceous aerosols. Two types of receptor-based models are extensively used to determine the origin of PM.

### *2.5.1 CMB model*

The CMB model is based on the principle of conservation of mass between the source and the receiver site considered. It permits to express the concentration of species *i* at the receptor site $C_i$ (in µg/m$^3$) as follows, which requires relatively few observations to be reliable,

$$C_i = \sum_{j=1}^{P} a_{ij} S_j , \qquad i = 1, \dots, n \qquad (2-1)$$

where $C_i$ is the concentration of species *i* measured at the receptor site in µg/m$^3$,

$a_{ij}$ is the mass fraction of species *i* in the profile of the source j (%),

*n* is the number of species,

$S_j$ is the mass concentration at the receptor site of all species assigned to the source *j* (µg/m$^3$).

$S_j$ is the contribution of a source at the receptor site, which could be determined through the application of CMB model. Therefore, the constraint of using such a model is the need to know precisely the emission sources profiles. The number of selected chemical species to describe the sources profile must be greater than the number of sources.

The effective variance weighted least squares minimization solution (Watson et al., 1984) is most commonly used for obtaining source contribution estimates ($S_j$), as implemented with CMB8 software (Watson et al., 1998).

CMB receptor model expresses concentrations of different chemical species measured at a monitoring site (or “receptor”) as a linear sum of products of source profile abundances and source contribution estimates. Source profile abundances are the mass fraction of a chemical or other property in the emissions from each source type that might contribute. Profiles are measured on samples from these sources at times and places believed to represent emissions compositions while receptor measurements are made. Differences in fuels and operating conditions are sought in these tests so that averages and standard deviations of the chemical abundances can be determined.

The elemental composition of the sources, especially metals, was once used for this purpose, but a large number of sources that produce particulate matter do not have emissions that contain only elemental components but emit large amounts of organic compounds and elemental carbon (Schauer et al., 1996).

Another aspect of the receptor-oriented source apportionment work is the identification and quantification of the organic tracer compounds collected at the receptor site. It is worthy to note that Schauer and Cass (2000) have developed molecular marker CMB models, which require measurements of organic tracers having unique association with specific sources of atmospheric fine particulate matter. These organic tracers have been identified for sources including wood smoke, mobile sources, road dust, and biomass burning as well as secondary organic aerosol formation (Schauer and Cass, 2000). A disadvantage with CMB source apportionment is the requirement of a priori knowledge of the source profiles. When CMB model is applied, it assumes that the composition of all sources is well defined and known. This technique is ideal when changes between the source and the receptor are minimal, although this barely happens in

real atmospheric conditions and the constraints may add a high level of uncertainty. To this end, questions are always raised with CMB models as to the accuracy of the source profiles and the ability to quantify errors associated with using source profiles that may not be representative of the sources impacting receptor sites.

### *2.5.2 PMF model*

Positive matrix factorization (PMF) is a factor analysis method that utilizes non-negativity constraints for the analysis of environmental data and associated error estimates. PMF solves the mass balance equations for each observation $x_{ij}$ made for the *j*-th species on the *i*-th day. The model assumes factor profiles $f_{kj}$ consisting of the *j*-th species in the *k*-th factor, and factor contributions $g_{ik}$ consisting of the *k*-th factor on the *i*-th day. Mathematically stated, the mass balance equation is as follows:

$$X_{ij} = \sum_{k=1}^{P} g_{ik} f_{kj} + e_{ij} \qquad (2-2)$$

where $e_{ij}$ is the residual concentration for each observation.

The model requires data for all concentration and uncertainty values for all *j* species and *i* days. Positive matrix factorization (PMF) does not require source profiles as model inputs but it does require knowledge of source profiles to determine the relationship of factors derived from the model with air pollution sources. Although PMF do not use source profiles as input data, it is untrue that source profiles are unnecessary for these models. PMF model derive source factors that must be associated with measured source profiles to achieve reliable source apportionment result.

The PMF source apportionment analysis requires an assumption of the number of significant factors affecting the monitored data. Because robust PMF analysis typically uses at least 60-200 required sets of observations, the model has typically been driven by trace elements, EC/OC measurements, and secondary inorganic ions, which are less specific than the molecular markers which were included in CMB source apportionment study (Jaeckels et al., 2007). Recently, Pekney et al. (2006) enhanced their analysis by including organic markers into the PMF model. A few organic compounds have been shown to be effective source indicators, including hopanes for vehicle exhaust, levoglucosan for vegetative burning. When these markers applied in PMF model to identify the sources of $PM_{2.5}$ in Pittsburgh, the primary OC/EC factor can be split into two factors: one associated with vehicle exhaust and road dust, and the other associated with vegetative burning, cooking, and vegetative detritus. These two factors usually cannot be separated based only on elemental, ionic, and thermal C fraction measurements.

Although these receptor models are becoming more and more widely used by researchers and regulators, there have been very limited studies to validate these models and evaluate the uncertainty with the model calculation. We noticed that Jaeckels et al. (2007) directly compared the use of molecular markers in CMB and PMF over two year period at the St. Louis Midwest Supersite and gained insight into the uncertainties of these source apportionment applications. In the context of the goals of source apportionment, the two models agree reasonably well and provide an important baseline to better evaluate the accuracy and biases of the source apportionment models. Therefore, it is needed to implement inter-comparison efforts among receptor-based models, thereby better understanding the source types and source contributions of airborne PM at receptor site.

### *2.5.3 PCA*

One commonly used multivariate receptor model is Principal Component Analysis (PCA). It has been successfully applied to identify sources in several studies (Lu et al., 2011; Eder et al., 2014). PCA is a statistical technique that transforms the original set of inter-correlated variables into a new set of independent principal components. Since PCA can be used to reduce dimensionality, the number of extracted principal components is usually smaller than that of original variables. In other words, PCA finds linear combinations of variables that describe major trends in a data set. Mathematically, PCA relies on eigenvalue decomposition of the covariance or the correlation matrix.

In PCA application, it supposes that several air pollutants were measured at a receptor site for long periods of time. The results then form a multivariate data set which contains concentrations of several pollutants in several ambient measurements. PCA simply suggests that ambient concentrations of pollutants involve fingerprints of sources that they have been emitted from, and these fingerprints can be extracted from the data set (Seinfeld and Pandis, 1998). The application of this method for interpretation of the complex databases permits understanding of the air quality in the study area, especially for developing suitable plans for management of the air quality monitoring programs and control strategies for air pollution.

However, the source apportionment of air pollutants using a simple mathematical analysis faces various challenges. One major drawback of PCA is that it is not a way to quantitatively estimate the source contributions to ambient pollutant concentrations.

# Chapter 3 Methodology

## 3.1 Sampling sites and descriptions

For a representative air quality in China, four sampling sites in this study were chosen at Wuqing, Haining, Zhongshan, Deyang, respectively. The four sites were located in four satellite cities of their corresponding megacities Beijing, Shanghai, Guangzhou, Chengdu, and approximate 100 kilometers away from the megacities (Figure 3-1).

Previous studies indicated that there are four major black carbon (BC) emission areas in China (Cao et al., 2006; Xing et al., 2014). They are Beijing-Tianjin-Hebei area (BTH), Yangtze River Delta area (YRD), Pearl River Delta area (PRD) and Sichuan Basin area (SB). The chosen sites in this study are within major black carbon (BC) emission areas in China.

The meteorological data over the last few years indicated that the chosen sites locate on the dispersion path of air mass from their corresponding megacities. Therefore, $PM_{2.5}$ collected at these sites could represent overall aged aerosol from corresponding megacities and are free from individual pollution plume.

Wuqing (39º39’N, 117º39’E) is located between Beijing and Tianjin. Since ancient times it serves as a transport hub and is known as the "Beijing-Tianjin corridor. Wuqing is 80 km away from Beijing downtown. It has a population of 0.84 million. The Wuqing landscape is mostly flat and riches with vegetation. Wuqing also has four distinct seasons.

Haining (30º51’N, 120º69’E) is a county-level city in Zhejiang Province, China. It is in the south side of Yangtze River Delta, and in the north of Zhejiang. It is 125 km west of Shanghai. The city has a population of 0.81 million. Haining is known for its leather industry and spectacular tide in the Qiantang River.


Figure 3-1 Location of four sampling sites in China

Zhongshan (22º56'N, 113º33'E) is a city located in Guangdong province with the population of around 3 million. It is located along the west side of the estuary of the Pearl River, 64 km away from Guangzhou, China. Zhongshan's climate is warm and humid most of the year, with an average temperature of 22 °C and 175 centimetres of rainfall each year. It experiences fairly frequent typhoons and thunderstorms, and most rain falls between April and September.

Deyang (31º10'N, 104º39'E) is located in the northeast of the Chengdu Plain in central Sichuan

Province, 66 km away from Chengdu, China. Deyang is a high-tech industrial city with the population of around 3.8 million. Major industry sector includes manufacturing, pharmaceuticals, chemicals, food, construction materials, and textiles. The city has a subtropical humid monsoon climate bearing obvious features of continental climate. The weather is humid with clear four seasons and abundant in rainfall during the period from May to October.

### 3.2 Sample collection

Atmospheric $PM_{2.5}$ samples were collected at four sites located in Wuqing, Haining, Zhongshan, Deyang in China during the period in November 2012, January 2013, April 2013 and July 2013. Daily samples were collected continuously for one week during each season of a year. Aerosol $PM_{2.5}$ samples were collected on quartz fiber filters (Φ90 mm, Millipore) at a flow rate of 100 L/min with approximate 24 hours on the roofs of the buildings with the height of about 10-30 meters using a medium volume air sampler (TH-150C III, Tianhong, Wuhan, China) with a $PM_{2.5}$ impactor (TH-$PM_{2.5}$-100, Tianhong, Wuhan, China). After sampling, the quartz filters were immediately placed in pre-baked aluminum foil and then stored frozen at -18 $^{o}$C until analyzed.

### 3.3 Chemical analysis

Blank and sample filters were weighed on an electronic balance (Sartorius-BT125D, Germany) with a reading precision of 0.01 mg to determine the aerosol mass concentration after its having been equilibrated at 25±0.5 $^{o}$C and 40±5 % relative humidity for 24 h. To better understand the detailed composition of fine PM in China, the chemical analysis of $PM_{2.5}$ samples in this study

includes water-soluble ions, carbonaceous components EC and OC, organic compounds.

### *3.3.1 water-soluble ions*

The collected aerosol $PM_{2.5}$ filter was ultrasonically extracted with 20 mL Milli-Q water (18.2 MΩcm) for 40 min. Then the extracted solution was filtered through 0.45 μm PTFE syringe filter (Pall Co. Ltd, USA). Analysis of extracted solutions was performed with an ion chromatograph (Metrohm, Switzerland) equipped with a conductivity detector. The concentrations of water-soluble components including five cations ($NH_4^+$, $Na^+$, $K^+$, $Ca^{2+}$, $Mg^{2+}$) and four anions ($F^-$, $Cl^-$, $NO_3^-$, $SO_4^{2-}$) were determined in this study. Quality assurance and quality control tests including field blank, laboratory blank, method detection limit, and recovery efficiency were conducted. Multi-point calibrations using standard solutions were carried out, and the result of correlation coefficient was higher than 0.999. All the reported ion concentrations have been corrected using field blanks.

### *3.3.2 carbonaceous components EC and OC*

The concentrations of organic carbon (OC) and elemental carbon (EC) were measured using a Sunset Carbon Aerosol Analyzer (Sunset Laboratory Inc., USA), following the NIOSH TOT protocol and assuming carbonate carbon in the sample to be negligible. Typically, a 1.5 $cm^2$ punch of the filter was placed in a quartz boat inside the thermal desorption chamber of the analyzer, and then stepwise heating was applied (Schauer and Cass, 2000).

### *3.3.3 organic compounds*

One half of each filter was cut into small species and then extracted twice with dichloromethane (TEDIA) and twice with methanol (ACROS) using an ultrasonic bath, followed by a rotary evaporator to concentrate the extracts to about 5 mL. The mixture of isotopically labeled compounds was spiked into each sample prior to extraction. The extracts were further blown down to reduce the volume to 0.5 mL under high-purity nitrogen (99.99 %). Each extract was split into two fractions, and a half of extracts were derivatized by BSTFA/TMCS 99:1 (Regis Technologies, Inc. USA) in sealed vials at 70 °C for 2 h to convert organic acids to their silylated analogues. Organic speciation was conducted using gas chromatography mass spectrometry (Agilent Technologies GC-6890, MS-5973).

One microliter of derivatized extracts was injected into GC-MS for identification and quantification of organic species. GC fitted with a fused silica capillary column (DB-5, 30 m, 0.25 mm i.d., 0.25 μm film thickness) and its condition was: initially, isothermal hold at 60 °C for 5 mins, temperature ramp of 5 °C/min to 300 °C, isothermal hold at 300 °C for 30 mins. The pure helium (99.999 % purity) is used as a carrier gas with a flow rate of 1.0 mL/min. The interface temperature of GC/MS was maintained at 300 °C. Organic compounds were ionized by electron impact (70 eV) and scanned from 50 amu to 550 amu in MS. The GC-MS data were acquired and analyzed by an Agilent Chemstation. According to GC retention times, MS spectrum and prepared authentic standards, individual organic compounds were identified and quantified, including alkanes, organic acids, polycyclic aromatic hydrocarbons (PAHs), and some molecular tracer compounds such as levoglucosan, hopanes, and steranes.

Filter blanks and solvent blanks throughout the field campaign and laboratory measurement, and duplicate samples analysis were performed for about 10 % of all $PM_{2.5}$ samples according to standard operating procedures. Spike recoveries of authentic standards were found in the range of 85% ~ 118%. All concentrations were blank corrected, and uncertainties were estimated on the basis of the standard deviation of field blanks and detection limit of the instruments.

### 3.4 Air mass transport model

In order to characterize the origin and transport pathway of the air masses to the sampling sites, back trajectory simulation was performed by using Hybrid Single-Particle Lagrangian Integrated Trajectory (HYSPLIT) model developed by NOAA/ARL (Draxler and Hess, 1998). 72-h back trajectories were calculated using the HYSPLIT model with an endpoint height of 500 m, 1000 m, and 1500 m, respectively. The meteorological data used for back trajectory simulation are six-hourly archived data from GDAS (Global Data Assimilation System) of NCEP (National Centers for Environmental Prediction).

### 3.5 Source apportionment model

Using molecular marker-based chemical mass balance (MM-CMB) approach, the specific source contributions to ambient OC and $PM_{2.5}$ mass concentrations were determined by calculating linear combination of the product of source effluents and its concentrations of a set of chemical species in ambient aerosol (Schauer et al., 1996; Watson et al., 1984). The organic compounds selected as tracers in the model should be chemically stable and conserved during transport from sources to receptor sampling sites, and all main sources were included in the model (Schauer et

al., 1996). The species selected for use in the present study were based upon the recommendations of previous studies (Lough et al., 2007; Schauer and Cass, 2000). Twenty one fitting species were included in the model, consisting of a continuous series of n-alkanes from $C_{25}$-$C_{33}$, levoglucosan, αββ-20R-$C_{27}$-cholestane, αββ-20R-$C_{29}$-sitostane, 17α(H)-21 β(H)-hopane, 17α(H)-22,29,30-Trinorhopane, 17β(H)-21α(H)-30-norhopane, benzo(e)pyrene, benzo(b) fluoranthene, benzo(k)fluranthene, indeno(1,2,3-cd)pyrene, benzo(ghi)perylene and picene. The picene, specific to coal combustion (Oros and Simoneit, 2000), was selected to infer whether coal combustion is a major contributor to ambient OC (Stone et al., 2008). The series of n-alkanes from $C_{25}$-$C_{33}$ were used to distinguish the biogenic and anthropogenic contributors according to carbon preference index (CPI). The hopanes and steranes were included to estimate the contributions from the combustion of fossil fuels (Manchester-Neesvig et al., 2003).

The source profiles used in this study were mainly obtained from US recent and comprehensive studies since fully constructed the local source profiles for these sites in China were not available. These source profiles included: woodsmoke (Fine et al., 2004; Sheesley et al., 2007), vegetative detritus (Rogge et al., 1993), diesel emission (Lough et al., 2007), gasoline vehicle (Lough et al., 2007), meat cooking (Rogge et al., 1991). Meanwhile, the coal combustion profile was obtained from measurement of particulate carbon emissions from real-world Chinese coal combustion experiment (Zhang et al., 2008). In addition, the criteria for acceptable CMB results included the square regression coefficient $R^2>0.85$, the sum of residual square value $CHI^2<4$, the degree of the freedom DF>5, and the percentage of explained mass to total mass ranging from 80 to 120 %.

# Chapter 4 Seasonal Variation and Sources of Water-Soluble Ions and Carbonaceous Fractions in $PM_{2.5}$

## 4.1 Introduction

Atmospheric aerosols consist of a mixture of suspended solid and liquid particles ranging over a few orders of magnitudes in sizes from natural or anthropogenic origin (Seinfeld and Pandis, 2006). The chemical composition of aerosol particles depends on multiple factors including primary emission source as well as post-formation processes. In general, water-soluble ions and carbonaceous components comprise a significant fraction of the ambient aerosol mass and influence the climate, visibility and human health through aerosol direct or indirect effects (Jacobson et al., 2000; Putaud et al., 2004; Raizenne et al., 1996).

The atmosphere in China has been increasingly contaminated by anthropogenic gases and aerosols due to fast industrialization and urbanization in the past decades. Recently, most of the megacities in China suffered haze pollution with severe atmospheric visibility degradation, which was mainly due to light extinction effects of fine aerosols in the atmosphere. Previous studies revealed that Beijing-Tianjin-Hebei area (BTH), Yangtze River Delta area (YRD), Pearl River Delta area (PRD) and Sichuan Basin area (SB) are the four major black carbon (BC) emission areas in China (Cao et al., 2006; Xing et al., 2014). Black carbon contributes to visibility impairment by efficiently absorbing light. In contrast, water-soluble inorganic ions such as $SO_4^{2-}$ and $NO_3^-$ were generally considered to be the major chemical species that contribute to the visibility reduction via light scattering effect. Although a number of studies concerning inorganic ions in aerosol have been conducted in China (He et al., 2001; Hu et al.,

2002; Wang et al., 2002; Wang et al., 2006; Shen et al., 2009; Pathak et al., 2009; Tan et al., 2009; Cao et al., 2012), they mainly focused on individual large cities or seasons. Due to the complexity of air pollution in nature and limitations of each individual analytical approach, the conclusions are sometimes perplexing and even contradicting (Zhang et al. 2013).Therefore, characterizing aerosol chemical compositions at large spatial scale in China using multiple analytical techniques are necessary to evaluate aerosols' effects on atmospheric visibility, human health, and climate change. In this study, we conducted a year-round sampling campaign at four key emission regions and investigated the effects of sources and long-range transportation by analyzing the ionic component, OC/EC, organic molecular markers, and carbon isotope. In this chapter, we focused on seasonal characterization of $PM_{2.5}$ ionic and carbonaceous components at four regional sites that have large pollution footprint to investigate the impact of potential sources and long-range transportation on regional air quality.

The four sites were located in four satellite cities of their corresponding megacities Beijing, Shanghai, Guangzhou, Chengdu, and approximate 100 kilometers away from the megacities. The sites are within major black carbon (BC) emission areas in China. Daily samples were collected continuously for one week during each season of a year. The meteorological data over the last few years indicated that the chosen sites locate on the dispersion path of air mass from their corresponding megacities. Therefore, $PM_{2.5}$ collected at these sites could represent overall aged aerosol from corresponding megacities and are free from individual pollution plume. The objectives of this work are to investigate the seasonal variations of water-soluble ions and carbonaceous components in $PM_{2.5}$ at four sites of China and reveal their potential sources and transport processes. The results presented here would shed light on some major factors

determining the distributions of major chemical components in $PM_{2.5}$ aerosol which is useful for making effective strategies for regional air quality improvement in China.

### 4.2 Characterization of $PM_{2.5}$ and major components

Table 4-1 presented a summary of statistics of water-soluble ions as well as EC, OC in $PM_{2.5}$ over the sampling period. The annual average $PM_{2.5}$ mass concentrations at Wuqing, Haining, Zhongshan, Deyang sampling sites were 148.9±91.1 μg $m^{-3}$, 109.6±59.4μg $m^{-3}$, 60.5±46.5 μg $m^{-3}$, and 121.5±101.1 μg $m^{-3}$, respectively. It is note that relatively high standard deviation is due to large seasonal variation of $PM_{2.5}$ in the whole year.

**Table 4-1** Summary of water-soluble ions, OC, EC in $PM_{2.5}$ at four cities of China

| Parameter/Species (Mean±SD μg $m^{-3}$) | Wuqing, Tianjin | Haining, Zhejiang | Zhongshan, Guangdong | Deyang, Sichuan |
|---|---|---|---|---|
| $PM_{2.5}$ | 148.9±91.1 | 109.6±59.4 | 60.5±46.5 | 121.5±101.1 |
| $NH_4^+$ | 8.5±5.9 | 6.1±4.3 | 2.8±2.8 | 6.3±6.4 |
| $Na^+$ | 0.5±0.3 | 0.3±0.2 | 0.3±0.3 | 0.3±0.3 |
| $Ca^{2+}$ | 0.9±0.8 | 0.4±0.2 | 0.3±0.2 | 0.5±0.3 |
| $Mg^{2+}$ | 0.2±0.1 | 0.2±0.0 | 0.1±0.0 | 0.2±0.1 |
| $K^+$ | 3.9±3.3 | 2.1±1.6 | 1.4±1.8 | 2.7±3.1 |
| $F^-$ | 0.4±0.2 | 0.2±0.1 | 0.1±0.1 | 0.1±0.2 |
| $Cl^-$ | 6.0±5.1 | 2.3±1.8 | 1.2±1.1 | 2.0±2.0 |
| $NO_3^-$ | 19.6±16.5 | 13.9±12.0 | 6.4±7.7 | 10.2±12.7 |
| $SO_4^{2-}$ | 24.2±21.8 | 16.5±9.9 | 9.8±6.3 | 21.6±18.3 |
| Total ions/$PM_{2.5}$ | 0.41±0.18 | 0.37±0.10 | 0.33±0.12 | 0.35±0.06 |
| OC | 14.1±13.8 | 9.0±3.7 | 7.0±5.0 | 13.8±13.2 |
| EC | 1.6±0.5 | 1.4±0.5 | 1.2±0.6 | 1.4±0.7 |
| TC | 15.7±14.1 | 10.3±3.9 | 8.2±5.5 | 15.1±13.7 |
| TC/$PM_{2.5}$ | 0.10±0.04 | 0.11±0.04 | 0.15±0.04 | 0.13±0.04 |
| Carbonaceous PM/$PM_{2.5}$ | 0.16±0.06 | 0.17±0.07 | 0.23±0.05 | 0.20±0.07 |

The $PM_{2.5}$ mass concentration in this campaign is comparable to those measured in other Chinese cities (Wang et al., 2005; Tao et al., 2014; Zhang et al., 2011; Hu et al., 2014) and India site (Verma et al. 2010), however its value is much higher than the new National Ambient Air Quality Standards of China for annual $PM_{2.5}$ (35 μg $m^{-3}$). As can be seen from the Table 4-1, sulfate was the most abundant water-soluble species. The concentrations of individual ions were in the order of $SO_4^{2-} > NO_3^- > NH_4^+ > K^+ > Na^+ > Mg^{2+}$, respectively. On average, nine water-soluble ions together contributed 33–41% of the $PM_{2.5}$ mass. Meanwhile, the carbonaceous matter was also found as a major component in $PM_{2.5}$ aerosol. The average total carbon (OC+EC) accounted for 10–15% of $PM_{2.5}$ mass during the campaign period. Assuming that the ratio of organic matter (OM) to OC was 1.6 (Turpin and Lim, 2001), the total carbonaceous particle matter (OM+EC) can be estimated, and it approximately comprised 16-23% of the $PM_{2.5}$ mass. It is worthy to note that the OM in this study might be underestimated especially during the warmer seasons when the fractions of secondary organic components and biological material are very high (Hueglin et al., 2005). The $PM_{2.5}$ aerosol at Wuqing site is characterized by higher water-soluble inorganic ions and lower OM composition. In contrast, fine aerosol at Zhongshan site showed higher relative abundance of OM particles whereas lower water-soluble ions.

### 4.3 Seasonal variation of water-soluble ions

The seasonal variation of $PM_{2.5}$ and major constituents at four sites in China are shown in Figure 4-1. The annual average $SO_4^{2-}$ concentration ranged from 9.8 to 24.2 μg $m^{-3}$ at four sites, accounting for 38-49 % of the total mass of water-soluble ions. Specifically, Wuqing site

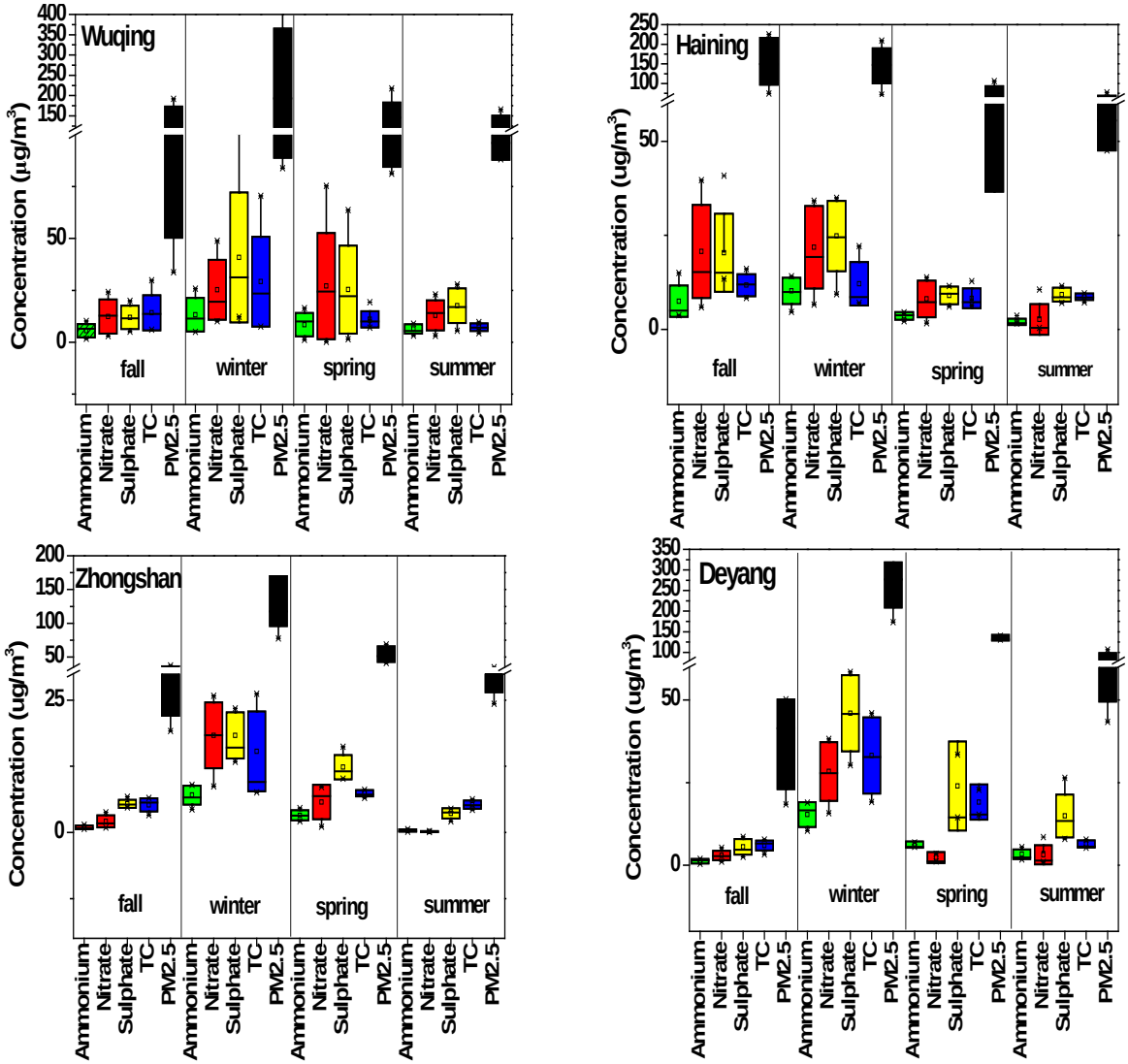


Figure 4-1 Seasonal variation of $PM_{2.5}$ and major constituents at four sites of China

suffered from the highest loading of water-soluble ions, while Zhongshan site recorded the lowest. The sulfate aerosols are mainly produced by chemical reactions of gaseous precursors (i.e. $SO_2$ gas from anthropogenic sources, dimethyl sulfide from oceans), which occur either in the gas phase with the OH radical or in cloud droplets with hydrogen peroxide ($H_2O_2$) or ozone (Pandis et al., 1990). The seasonal variation of sulfate was obvious and slightly different

temporal trend was found among these sites. In general, sulfate showed the highest concentration in winter. Such high level of $SO_4^{2-}$ in winter is likely due to anthropogenic emissions (i.e. coal combustion) coupled with poor dispersion condition during the cold season (He et al., 2001). It is noticed that summer samples at Wuqing and Deyang showed an elevated level of sulfate with respect to fall. As secondary ion in fine aerosol, $SO_4^{2-}$ might be caused by enhanced photochemical reaction and aqueous processing at high temperature, intensive solar radiation, and high relative humidity.

The annual concentration of $NO_3^-$ varied from 6.4 to 19.6 μg $m^{-3}$, and it contributed to 23-33% of total mass of water-soluble ions. The seasonal variations of $NO_3^-$ are characterized by winter/spring maxima and summer minima at these sites. These findings were consistent with those reported in other Chinese cities (Duan et al., 2006; Hu et al., 2008; Cao et al., 2012). The nitrate aerosol is formed through heterogeneous reactions of nitrogen radicals such as NOx, and $HNO_3$ on aerosol surfaces (Bauer et al., 2007), depending mainly on the thermodynamic state of its precursor and the environmental conditions such as atmospheric temperature and relative humidity (Lin et al., 2010). The highest values of nitrate measured in winter might be ascribed to local pollution sources, such as vehicular traffic (Paraskevopoulou et al., 2015). Meanwhile, the low temperature in winter and spring is beneficial to the formation of nitrate aerosol.

The annual concentration of $NH_4^+$ varied from 2.8 to 8.5 μg $m^{-3}$, and it showed a strong seasonal cycle with peak values in winter/spring and relatively low in summer. $NH_4^+$ was observed as the most abundant cation in this study and contributed to 13-15% of total mass of water-soluble ions. Ammonium ($NH_4^+$) in the aerosol is produced from the reaction between $NH_3$ and acidic species present in either the gas or aerosol phase. In winter, lower temperature and higher acid species

such as sulfate and nitrate will favor the gas-particle reactions of $NH_3$ to $NH_4^+$ (Pathak et al., 2009; Meng et al., 2014). Compared to the other sites over the world, the $SO_4^{2-}$, $NO_3^-$, $NH_4^+$ concentrations observed in this study were higher than Athens, Greece (Paraskevopoulou et al., 2015) and Seoul, Korea (Shon et al., 2013) except Raipur, India (Verma et al., 2010).

### 4.4 Seasonal variation of carbonaceous matter

The yearly mean concentration of elemental carbon (EC) is 1.6 μg $m^{-3}$, 1.4 μg $m^{-3}$, 1.2 μg $m^{-3}$ and 1.4 μg $m^{-3}$ for sampling sites at Wuqing, Haining, Zhongshan, and Deyang, respectively (Figure 4-2). EC concentration exhibited least seasonal variability at these sites, suggesting a fairly uniform local source, i.e. primary particles from fossil fuel incomplete combustion. The OC concentration varied between 9.0 and 14.1 μg $m^{-3}$ at these sampling sites. The OC mass

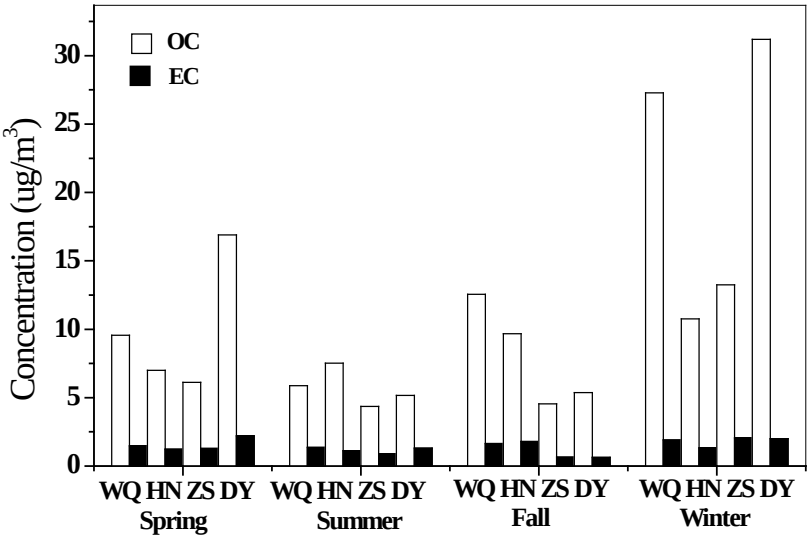


Figure 4-2 Seasonal variation of OC and EC in $PM_{2.5}$ at four sites of China.
Wuqing (WQ), Haining (HN), Zhongshan(ZS), Deyang(DY)

concentrations at Wuqing and Deyang sites are around 80% higher than those measured at Haining and Zhongshan sites. Furthermore, OC concentration showed strong seasonal variation with highest in winter, followed by fall and spring, and lowest in summer.

OC/EC ratios during this campaign period were found to be 3.0-27.9 with a mean of 5.8-8.9. These ratios are higher than those reported for the megacities in China (Yao et al., 2002; Cao et al., 2003; Ho et al., 2003). The high OC/EC ratios at these sites suggest that OC is largely produced by photochemical processes during long-range transport. Furthermore, secondary organic carbon (SOC) concentration was estimated with the EC-tracer method based on the following equation (Turpin and Huntzicker, 1995),

$$SOC=OC_{tot} - EC\times(OC/EC)_{pri} \qquad (4-1)$$

where $OC_{tot}$ is the total OC, and $(OC/EC)_{pri}$ is the primary OC/EC ratio.

It should be noted that some uncertainty in the estimation method since primary OC/EC emission ratio vary between sources and it is usually influenced by meteorology condition (Strader et al., 1999; Zhou et al., 2012). In this study, we selected data with OC/EC ratio in the lowest 10% to determine the primary OC/EC ratio, assuming that the primary OC/EC ratio can be determined during the periods in which conditions are highly unfavorable for the production of SOC. Primary OC/EC ratio of 2.2 was determined by least-square regression as the threshold value to estimate the concentration of SOC.

It is worthy to note that OC/EC ratios at Haining and Zhongshan sites observed highest in summer are likely due to the local photochemical production of secondary OC during the warm season. Actually, the contribution of SOC to the total OC ranged from 42.5 to 74.3% with an average of 62.5%, indicating that more SOA was formed through photochemical reaction during

summertime at these sites. Interestingly, the observations of increasing ratios of OC/EC (14.2-15.5) at Deyang and Wuqing sites during wintertime might be attributed to additional input of primary OC from different sources which enhance the OC value on transport pathway to these sites (Aggarwal and Kawamura, 2009). In fact, the high percentage of SOC/OC (61.2 to 78.9%) observed during wintertime was probably due to the biomass burning emissions because this source has much higher primary OC/EC ratio and can cause overestimation of SOC.

Table 4-2 listed the concentrations of $PM_{2.5}$, water-soluble ions, and carbonaceous species at different sites over the world. In this study, the concentrations of OC and EC are comparable to some urban sites in China, e.g. Chengdu (Tao et al., 2014), and much higher than Athens, Greece (Paraskevopoulou et al., 2015), however apparently lower than tropical pasture site in Rondônia, Brazil (Kundu et al., 2010).

### 4.5 Aerosol chemistry and ions balance

The molar ratios of cation equivalents (CE) and anion equivalents (AE) are frequently employed to infer the acidity of aerosol (Chow et al. 1994; Hennigan et al., 2015). At this study, ions balance was evaluated using the following equations.

$$CE = \frac{[Na^+]}{23} + \frac{[NH_4^+]}{18} + \frac{[K^+]}{39} + \frac{[Ca^{2+}]}{20} + \frac{[Mg^{2+}]}{12} \qquad (4-2)$$

$$AE = \frac{[SO_4^{2-}]}{48} + \frac{[NO_3^-]}{62} + \frac{[Cl^-]}{35.5} + \frac{[F^-]}{19} \qquad (4-3)$$

As shown in Figure 4-3, both anions and cations are strongly correlated, and the ratios of AE/CE were slightly higher than one, indicating the $PM_{2.5}$ aerosols at four sites were characterized by acidic in nature. It means the neutralization of sulfate and nitrate in aerosol was not completely

**Table 4-2** Comparison of $PM_{2.5}$, water-soluble ions and carbonaceous species at different sites over the world

| Location | Period | $PM_{2.5}$ μg $m^{-3}$ | OC μg $m^{-3}$ | EC μg $m^{-3}$ | $SO_4^{2-}$ μg $m^{-3}$ | $NO_3^-$ μg $m^{-3}$ | $NH_4^+$ μg $m^{-3}$ |
|---|---|---|---|---|---|---|---|
| Beijing, China [a] | 2001-2003 | 154.26± 145.65 | - | - | 17.07± 16.52 | 11.52± 11.37 | 8.72 ±7.66 |
| Chengdu, China [b] | 2011 | 119±56 | 17±8 | 7±4 | 25.0±14.1 | 10.7±7.8 | 11.6±7.3 |
| Xi'an, China [c] | 2006-2007 | 194.1±78.6 | - | - | 35.6±19.5 | 16.4±10.1 | 11.4±6.8 |
| Athens, Greece [d] | 2008-2013 | 20±11 | 2.1±1.3 | 0.54±0.39 | 3.1 ± 0. 8 | 0.45 ± 0.19 | 0.67± 0.26 |
| Seoul, Korea [e] | 2010 | 25.2± 19.0 | - | - | 5.19±4.58 | 12.3 ± 7.17 | 3.73± 3.59 |
| Raipur, India [f] | 2005-2006 | 167.0±75.3 | - | - | 46.5±32.8 | 8.2±7.1 | 8.8±7.7 |
| Rondônia, Brazil [g] | 2002 | - | 19.5-86.4 | 0.6–3.6 | 2.7 ± 0.3 | 2.1 ± 1.4 | 1.26± 0.51 |
| Four sites in China [h] | 2012-2013 | 60.5-148.9 | 7.0-14.1 | 1.2-1.6 | 9.8-24.2 | 6.4-19.6 | 2.8-8.5 |

[a] Wang et al. 2005
[b] Tao et al. 2014
[c] Zhang et al. 2011
[d] Paraskevopoulou et al. 2015
[e] Shon et al. 2013
[f] Verma et al. 2010
[g] Kundu et al. 2010
[h] This study

achieved at these sites. It is known that among the ammonium-associated compounds, $(NH_4)_2SO_4$ is preferentially formed due to its least volatility, while $NH_4NO_3$ is relatively volatile, and $NH_4Cl$ is the most volatile. Furthermore, the non-sea-salt fractions of sulfate (nss-$SO_4^{2-}$), potassium (nss-$K^+$) and calcium (nss-$Ca^{2+}$) were estimated with the following equations using measured sodium concentrations and the known ratios of each ion to $Na^+$ in the bulk sea water, assuming the soluble $Na^+$ in aerosol particulate comes only from sea-salts and sea-salts has the same chemical composition as the sea water (Morales et al., 1998; Harrison and van Grieken, 1998).

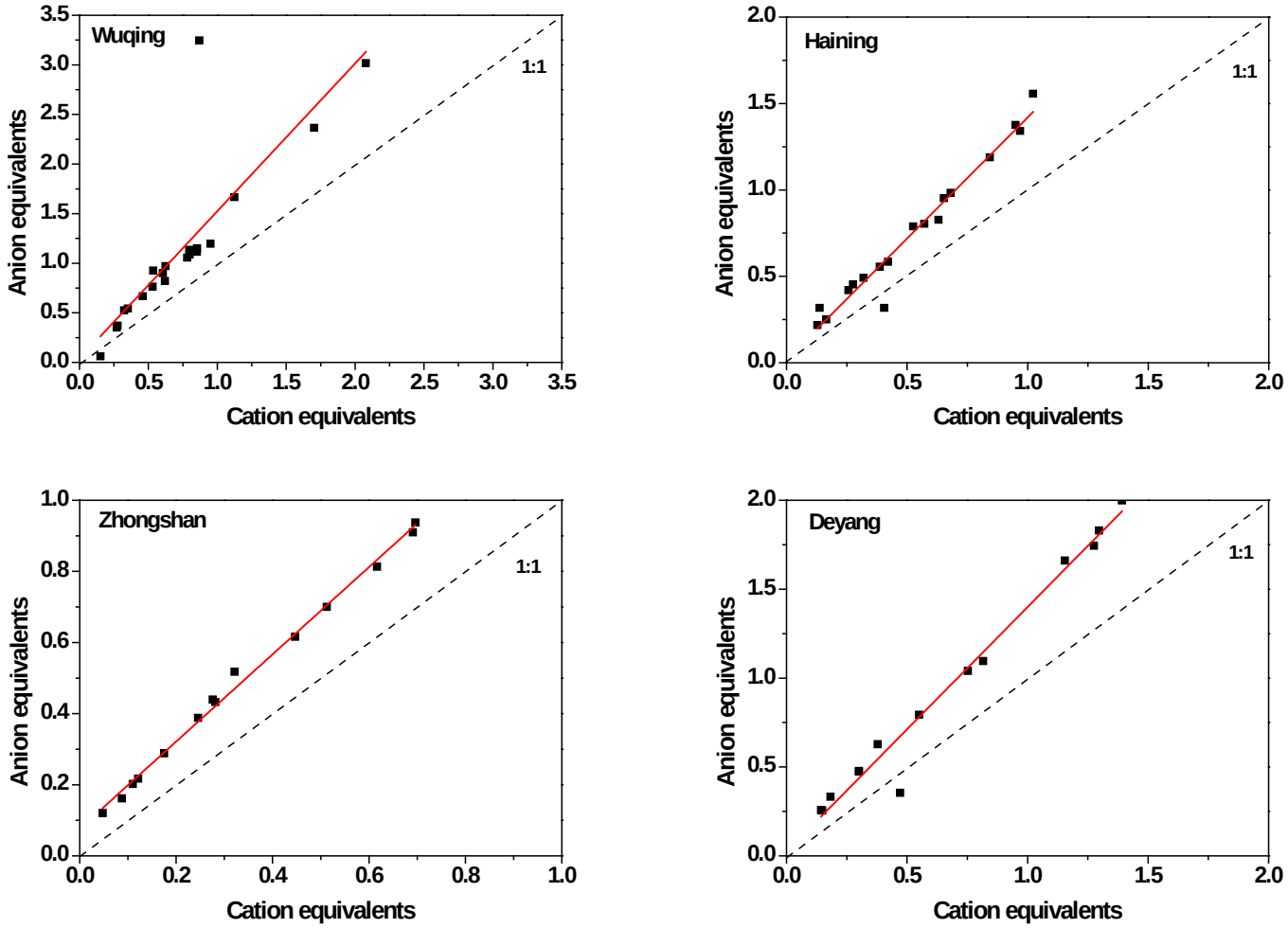


Figure 4-3 Correlations between anion equivalents and cation equivalents at four sampling sites

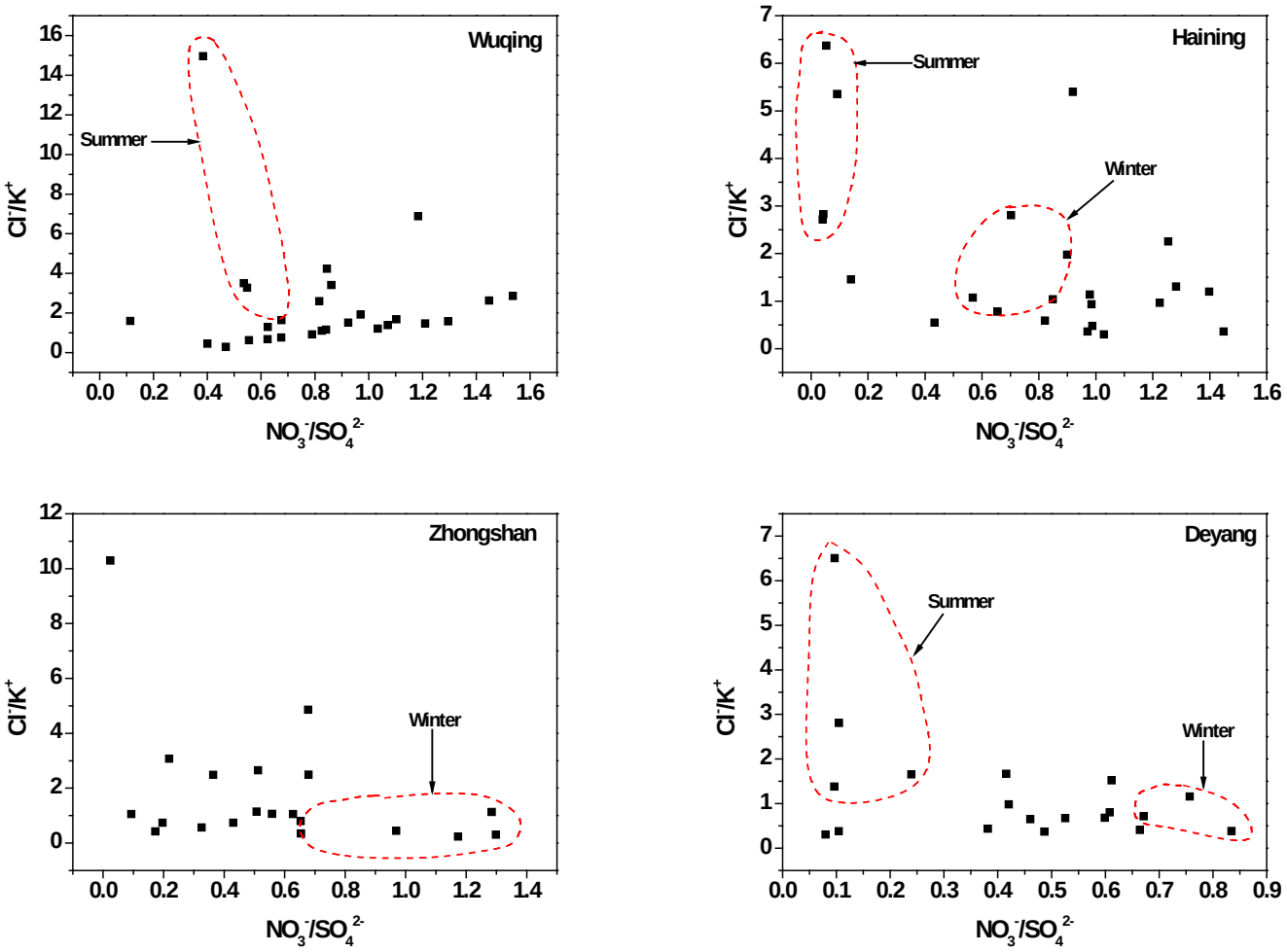


Figure 4-4 Relationship between $Cl^-/K^+$ and $NO_3^-/SO_4^{2-}$

$$nss\text{-}SO_4^{2-} = [SO_4^{2-}] - [Na^+] \times 0.2455 \quad (4—4)$$

$$nss\text{-}K^+ = [K^+] - [Na^+] \times 0.0355 \quad (4—5)$$

$$nss\text{-}Ca^{2+} = [Ca^{2+}] - [Na^+] \times 0.0373 \quad (4—6)$$

Under the ammonium-poor condition, the positive correlations between nss-$SO_4^{2-}$ and $NH_4^+$ (R=0.92-0.98) at a very significant level (P<0.001) revealed the sulfate aerosol primarily existed in the form of $(NH_4)_2SO_4$ in the atmosphere at these sites.

Previous studies showed that the mass ratio of nitrate/sulfate is generally used to evaluate the relative contribution of mobile and stationary sources in the atmosphere (Wang et al., 2005). The average mass ratios of $NO_3^-/SO_4^{2-}$ were 0.43, 0.57, 0.83, 0.93 for Deyang, Zhongshan, Wuqing, and Haining, respectively, suggesting that the stationary source emissions were predominant at these sites (Khoder and Hassan, 2008). Comparatively among the sites, Deyang has been influenced by more emissions from coal burning, whereas Haining received more loadings from vehicle emissions. Chloride ($Cl^-$) in coarse aerosol particles is mainly from marine source, and it might also accumulate in fine particulate originating from anthropogenic emissions such as coal combustion, biomass burning. Potassium ($K^+$) in fine mode aerosols is generally served as a diagnostic tracer for biomass burning source (Andreae et al., 1998). The ratios of $Cl^-/K^+$ at this study are relatively higher in summer with large variation, and lower in fall and winter (Figure 4-4). Since $K^+$ is steady, it remains in particulate phase once emitted from fire source. Thus its accumulation in the aerosol phase decreased the ratio of $Cl^-/K^+$ in the cold season. The emission of biomass burning in the cold season and regional long-range transport in summer are likely most responsible for this observation (Yin et al., 2014). It is worth noting that the highest ratios of $Cl^-/K^+$ were found at Wuqing site during summer might be associated with coal combustion (McCulloch et al., 1999). Similarly, ratios of $Cl^-/K^+$ ranging from 2.8 to 6.5 combined with ratios of $NO_3^-/SO_4^{2-}$ ranging between 0.1 and 0.2 confirmed the coal combustion emissions at Haining site during the summer period. Moreover, a significant increase in concentrations of $PM_{2.5}$ (116.4-135.4 μg $m^{-3}$)

coupled with high $Ca^{2+}$ (0.7-1.2 μg $m^{-3}$) were observed at Wuqing and Deyang sites during spring, implying these sites were affected by local emissions and continental dust through long-range transport.

### 4.6 Influence of air masses transport

72-h back trajectories were calculated by HYSPLIT model to get insight into the origin and transport pathway of the air masses arriving at these sites. As illustrated in Figure 4-5, the majority of the air masses during summertime reaching these sites were from western Pacific Ocean passing over Yangtze River Delta (YRD), Pearl River Delta (PRD) regions, whereas at Deyang site the air mass originated from southern mainland coupling with local Sichuan Basin (SB) emissions and long-range transport from South Asia. This is confirmed by the high concentration of $Na^{+}$ (0.2-0.3 μg $m^{-3}$) in marine air masses, while lower $Na^{+}$ values observed at Deyang on July 14, 2013.

Figure 4-6 showed that the dust originating in the Mongolia moved southeastward and mixed with air masses passing over North China Plain (Hebei Province and Shanxi Province), and finally arrived at Wuqing site during wintertime. The aerosol chemical data on January 18, 2013 is characterized by high level of $Ca^{2+}$ (1.3 μg $m^{-3}$) and $Mg^{2+}$ (0.2 μg $m^{-3}$), together with high concentration of $NO_3^{-}$ (25.2 μg $m^{-3}$), $SO_4^{2-}$ (40.9 μg $m^{-3}$), OC (27.3 μg $m^{-3}$), $K^{+}$ (7.2 μg $m^{-3}$), suggesting the polluted air masses on that day was mixed with fossil fuel combustion and continental dust via long-range transport.

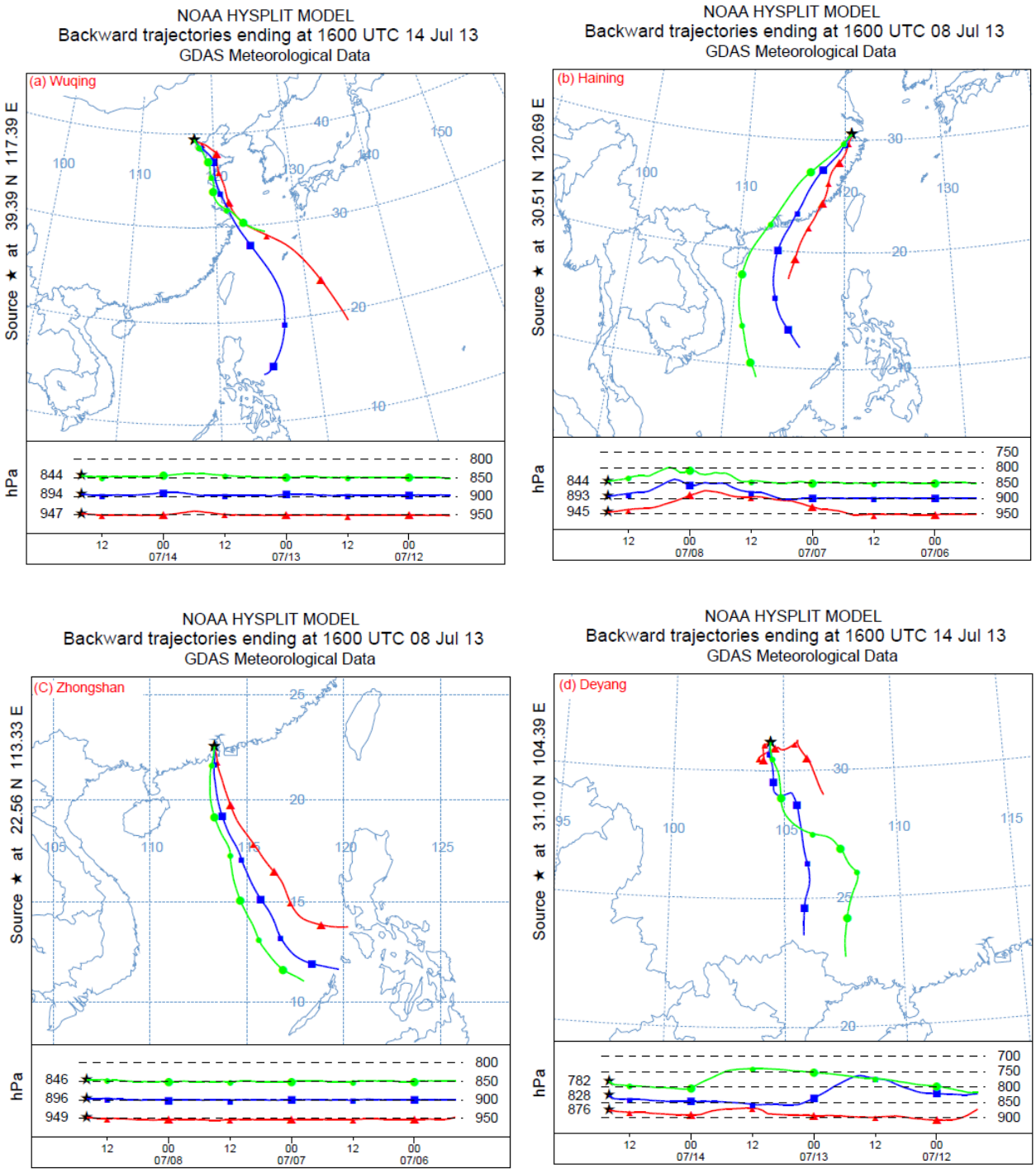


Figure 4-5 The 3-day back trajectories of air masses arriving at sampling sites in Wuqing (a), Haining (b), Zhongshan (c), Deyang (d) during summertime

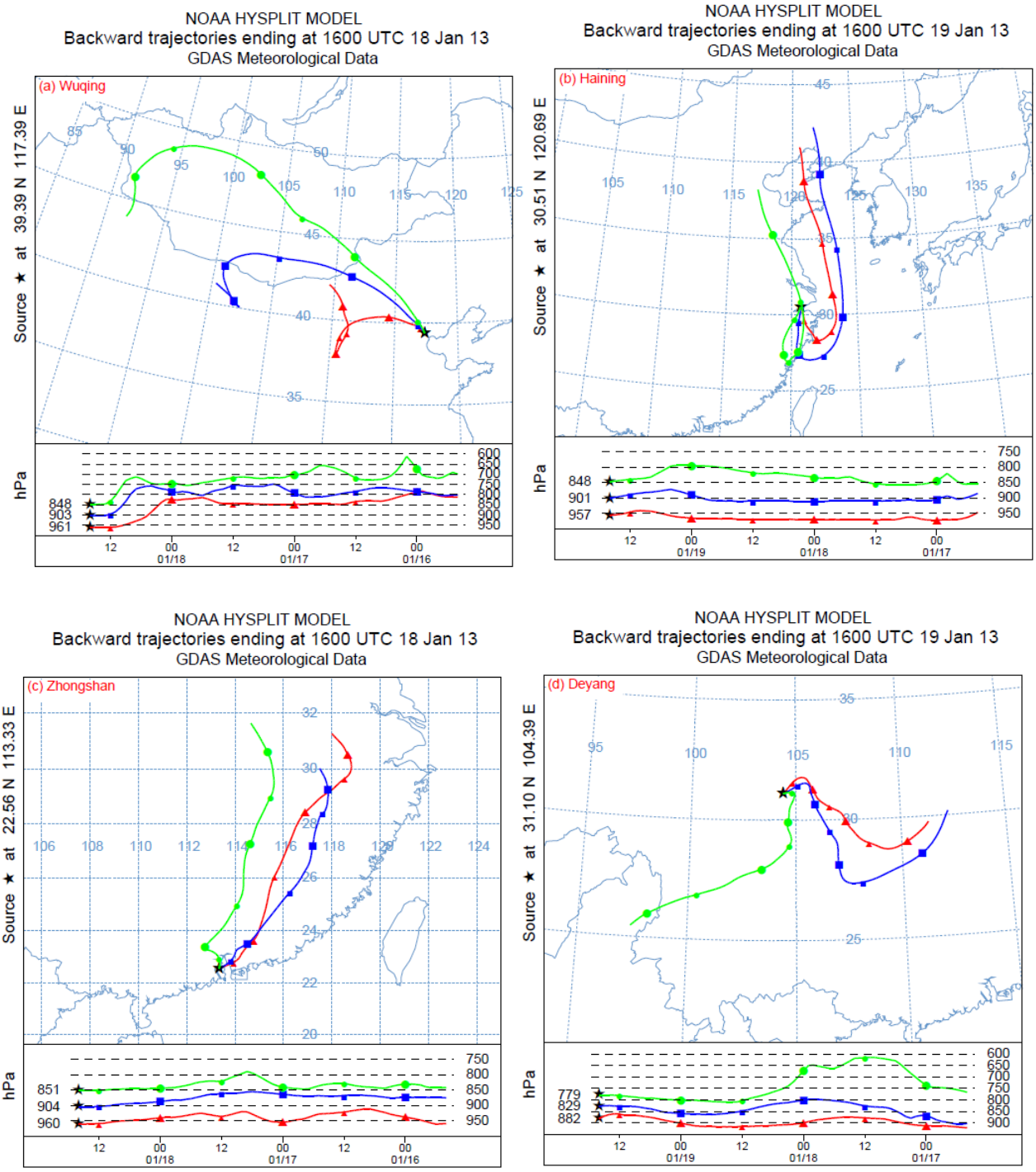


Figure 4-6 The 3-day back trajectories of air masses arriving at sampling sites in Wuqing (a), Haining (b), Zhongshan (c), Deyang (d) during wintertime

We noted that high correlation of $K^+$ with $SO_4^{2-}$ ($R^2$=0.90) during winter, hence $K^+$ may exist as $K_2SO_4$ which is often present in aged smoke especially when the aerosol in this campaign is acidic and ammonium-deficient (Li et al. 2003).

Meanwhile, air masses arrived at Deyang site on January 19, 2013, carrying high level of $SO_4^{2-}$ (46.0 μg $m^{-3}$), $NO_3^-$ (28.4 μg $m^{-3}$), $K^+$ (7.0 μg $m^{-3}$). It indicated that the aerosol was under the influence of fossil fuel combustion and biomass burning from both the lower part of atmospheric boundary layer (ABL) in Central China and long-range transport from South Asia (Figure 4-6). These results together suggest that both long-range transport and local sources have important impact on ions and carbonaceous particles in the aerosol at these sites.

It is worth noting that a haze event in eastern China was recorded in January 2013. The overall higher $SO_4^{2-}/PM_{2.5}$ ratios for Wuqing (0.18) compared with Haining and Zhongshan site during the winter sampling campaign indicate relatively higher coal combustion emission in North China Plain (NCP) region. In contrast, $NO_3^-/PM_{2.5}$ ratios at Haining and Zhongshan sites (0.13-0.15) in winter have been found to be significantly higher than in Wuqing, suggesting a relatively greater contribution from traffic emissions. Interestingly, the ratios of $K^+/ PM_{2.5}$ (0.02-0.03) varied little during winter among the four sites, which imply that these haze events were equally affected by biomass combustion in all four regions. The present results are in general agreement with the findings of Andersson et al. during the same study period which revealed that high coal contributions to EC in NCP region and more liquid fossil in YRD and PRD region using dual carbon isotope constrained ($\Delta^{14}C$ and $\delta^{13}C$) source apportionment method (Andersson et al., 2015).

### 4.7 Source identification of ions

In this study, principal component analysis (PCA) technique was applied with major aerosol data to identify the main contributions of processes and emission sources of water-soluble ions. Table 4-3

presented PCA results with varimax rotation using $PM_{2.5}$ chemical component data at four sites respectively. All principal factors with eigenvalues > 1 were extracted.

At Wuqing site, three principal components were extracted and accounted for 90% of the total variance. The principal component 1 had highly positive loading from $NH_4^+$ (0.942), $SO_4^{2-}$ (0.912), $K^+$ (0.934), nss-$SO_4^{2-}$ (0.911), nss-$K^+$ (0.934), OC (0.920), indicating industry source mixing with biomass burning. The principal component 2 is only characterized by $Cl^-$ (0.543), which can be related to coal combustion. Additionally, the principal component 3 is linked with a high value of $NO_3^-$ (0.543). It can be identified as vehicle emission.

We noted that the first component at Haining site is characterized by $NH_4^+$ (0.946), $K^+$ (0.929), nss-$K^+$ (0.929), suggesting likely origins from industry source mixing with biomass burning. The second factor, explaining 14.59% of the variance, had high factor loading for $Ca^{2+}$ (0.881) and nss-$Ca^{2+}$ (0.896), indicating the possible source from soil dust. The third factor is dominated by EC, which implies the component is associated with primary particles from incomplete combustion. The fourth factor with high loading for $Cl^-$ (0.558) and low loading for $Na^+$ (0.339) indicated the possible source from coal combustion.

Similarly, the principal component analysis performed on aerosol data set for Zhongshan site revealed industry source, soil dust, and coal/biomass combustion as the main source of the ions in $PM_{2.5}$. At Deyang site, water-soluble ionic components in $PM_{2.5}$ are possibly affected by industry source and soil dust. It is worth noting that the nss-$SO_4^{2-}$ together with OC had high loading on the first factor, which might be attributed to the secondary photochemical formation at this site.

**Table 4-3** Factor loading from PCA in $PM_{2.5}$ at four sites of China

| | Wuqing | | | Haining | | | |
|---|---|---|---|---|---|---|---|
| Species | PC1 | PC2 | PC3 | PC1 | PC2 | PC3 | PC4 |
| $NH_4^+$ | **0.942** | 0.075 | 0.077 | **0.946** | -0.038 | -0.276 | -0.089 |
| $Na^+$ | 0.876 | 0.028 | -0.354 | 0.848 | -0.283 | -0.156 | 0.339 |
| $Ca^{2+}$ | 0.715 | -0.592 | 0.33 | 0.371 | **0.881** | 0.049 | 0.253 |
| $Mg^{2+}$ | 0.875 | -0.33 | 0.049 | 0.611 | 0.293 | 0.497 | -0.099 |
| $K^+$ | **0.934** | 0.101 | -0.293 | **0.929** | -0.155 | 0.183 | -0.006 |
| $F^-$ | 0.679 | 0.027 | -0.531 | 0.366 | 0.064 | 0.303 | -0.699 |
| $Cl^-$ | 0.413 | **0.677** | 0.461 | 0.596 | -0.424 | 0.005 | **0.558** |
| $NO_3^-$ | 0.673 | 0.456 | **0.543** | 0.879 | 0.055 | -0.18 | -0.251 |
| $SO_4^{2-}$ | **0.912** | 0.043 | 0.291 | 0.878 | 0.033 | -0.405 | -0.209 |
| nss-$SO_4^{2-}$ | **0.911** | 0.043 | 0.292 | 0.877 | 0.034 | -0.406 | -0.211 |
| nss-$K^+$ | **0.934** | 0.101 | -0.293 | **0.929** | -0.155 | 0.184 | -0.008 |
| nss-$Ca^{2+}$ | 0.707 | -0.596 | 0.337 | 0.341 | **0.896** | 0.055 | 0.242 |
| OC | **0.920** | -0.159 | -0.258 | 0.655 | -0.079 | 0.3 | 0.347 |
| EC | 0.718 | 0.438 | -0.309 | 0.324 | -0.231 | **0.835** | -0.068 |
| % Variance | 66.283 | 12.349 | 11.786 | 52.166 | 14.59 | 11.865 | 9.507 |
| Probable source | Industry source | Coal combustion | Vehicle emission | Industry source | Soil dust | Incomplete combustion | Coal combustion |

| | Zhongshan | | | Deyang | |
|---|---|---|---|---|---|
| Species | PC1 | PC2 | PC3 | PC1 | PC2 |
| $NH_4^+$ | **0.973** | -0.088 | 0.127 | **0.975** | -0.162 |
| $Na^+$ | **0.946** | -0.141 | -0.245 | **0.956** | -0.141 |
| $Ca^{2+}$ | 0.282 | **0.936** | 0.181 | 0.614 | **0.766** |
| $Mg^{2+}$ | 0.489 | **0.802** | -0.12 | 0.873 | 0.156 |
| $K^+$ | **0.946** | -0.287 | -0.057 | **0.977** | -0.117 |
| $F^-$ | 0.505 | -0.181 | 0.18 | 0.898 | -0.279 |
| $Cl^-$ | 0.641 | 0.434 | **-0.574** | **0.937** | -0.019 |
| $NO_3^-$ | **0.945** | -0.141 | 0.029 | 0.896 | -0.333 |
| $SO_4^{2-}$ | **0.915** | -0.036 | 0.359 | **0.963** | -0.045 |
| nss-$SO_4^{2-}$ | **0.912** | -0.035 | 0.365 | **0.962** | -0.045 |
| nss-$K^+$ | **0.946** | -0.287 | -0.056 | **0.976** | -0.117 |
| nss-$Ca^{2+}$ | 0.245 | **0.945** | 0.192 | 0.585 | **0.787** |
| OC | 0.87 | -0.034 | -0.451 | **0.954** | -0.12 |
| EC | **0.961** | -0.088 | 0.16 | 0.565 | 0.395 |
| % Variance | 63.690 | 20.411 | 7.291 | 77.311 | 11.908 |
| Probable source | Industry source | Soil dust | Coal combustion | Industry source | Soil dust |

### 4.8 Summary

The seasonal variation of aerosol $PM_{2.5}$ and its ionic constituents as well as carbonaceous matter from four satellite city sites in China over a one-year period are presented. The annual average $PM_{2.5}$ mass concentrations ranged from 60.5 to 148.9 μg $m^{-3}$. On average, Wuqing site had the highest concentration of aerosol $PM_{2.5}$ and chemical species, followed by Deyang and Haining, while Zhongshan site was found being the lowest. The water-soluble ions were dominated by three ionic species ($SO_4^{2-}$, $NO_3^-$, $NH_4^+$) accounting for 33-41% of the $PM_{2.5}$ mass. In general, water-soluble ions exhibited a clear seasonal pattern with the highest concentration in winter while lowest in summer. Additionally, the total carbonaceous particle matter approximately comprised 16-23% of the $PM_{2.5}$ mass.

Ion balance calculations showed the aerosols at four sites were characterized by acidic in nature. The aerosol chemical composition combined with back trajectory analysis confirmed that both long-range transport and local emissions have important impact on ions and carbonaceous particles in the aerosol at these sites. PCA indicated that major sources of ions are vehicular emissions, coal/biomass combustion, industry source, as well as soil dust. This study provided us with valuable information on spatiotemporal variability of major chemical constituents in $PM_{2.5}$, and therefore will give a better understanding on the impact of aerosol chemical compositions on atmospheric visibility impairment during haze events in China.

# Chapter 5 Organic Composition and Source Apportionment of $PM_{2.5}$ in China

## 5.1 Introduction

Atmospheric aerosols have been shown to have pronounced effect on human health, visibility reduction and global climate (Charlson et al., 1992; Seinfeld and Pandis, 1998). The organic aerosol is a significant constituent of aerosol particles mass, comprising thousands of compounds with very different physical and chemical properties (Saxena and Hildemann, 1996). The complex nature of organic aerosol makes it difficult to fully characterize all organic compounds in the atmospheric particulate matter at the molecular level (Nolte, et al., 2002; Schauer, et al., 2002).

Primary organic aerosols (POA) are those emitted directly into the atmosphere in particle form, while secondary organic aerosols (SOA) are formed through the chemical reaction of biogenic and anthropogenic gaseous precursors. Biogenic volatile organic compounds have been positively identified as a precursor to the formation of SOA in the atmosphere (Kavouras et al., 1999; Jaoui and Kamens, 2003). Among the precursor substances, isoprene and terpenes are generally considered as the major producers to SOA (Kleindienst et al., 2006). Meanwhile, aromatic compounds have also the potential to form SOA (Odum et al., 1997). Note that these anthropogenic aromatics emissions in South and East Asia may have significantly increased during last three decades (Kanakidou, et al., 2005).

Currently, China is facing serious ambient particulate matter pollution as rapid economic development and urbanization. Previous studies revealed that Beijing-Tianjin-Hebei area (BTH), Yangtze River Delta area (YRD), Pearl River Delta area (PRD) and Sichuan Basin area (SB) are the four major black carbon (BC) emission areas in China (Cao et al., 2006; Xing et al., 2014). Herein, sampling sites (shown in Figure 3-1) were chosen in four satellite cities of their corresponding megacities Beijing, Shanghai, Guangzhou, and Chengdu, which was described in our previous paper (Zhou et al., 2016). To the best of our knowledge, only limited data on individual organic composition of aerosol particles is available in these areas.

The present study aims to compare the compositions of individual organic compound in $PM_{2.5}$ and to evaluate source contributions to OC and $PM_{2.5}$ mass using organic tracer-chemical mass balance (CMB) receptor model. The results of this study will be helpful for designing effective ambient particulate matter pollution control strategies and human exposure studies.

### 5.2 Organic species and source identification

The annual average OC concentration varied between 9.0 and 14.1 μg $m^{-3}$ at these sampling sites, while the EC concentrations were observed to be 1.2-1.6 μg $m^{-3}$. More than one hundred of organic compounds including alkanes, PAHs, n-alkanoic acids, aliphatic and aromatic dicarboxylic acids were identified and quantified in each sample. Among them, some molecular markers or indicator compounds were well documented as the tracers to the source of organic matter (Simoneit, 1985). In this work, some selected organic molecular markers in $PM_{2.5}$ including hopanes, picene, high-molecular-weight (HMW) PAHs, levoglucosan, cholesterol, dicarboxylic acids are presented in Figure 5-1.

Hopanes, petroleum biomarkers, are commonly utilized to as tracers for motor vehicle exhaust in the atmosphere (Rogge et al., 1993; Schauer et al., 2000). As shown in Figure 5-1a, the hopanes including 17α(H)-22,29,30-Trisnorhopane, 17α(H),21β(H)-30-Norhopane, 17α(H),21β(H)-Hopane contributed to $PM_{2.5}$ mass with an annual average concentration (±sd) of 2.3±1.8 ng $m^{-3}$. The maximum values at these sites were observed in fall and winter and the minimum values were in spring, except highest level occurred at Deyang during the summer period. The hopanes in the aerosol confirmed the input source from fossil fuel utilization and engine lubricating oil at these sites.

The concentrations of picene, a tracer for coal combustion, was found the highest value in winter and lowest in summer with an annual average of 0.2±0.1 ng $m^{-3}$ (Figure 5-1b). Wuqing site exhibited much

higher picene level than that at Zhongshan site. The maximum value occurred in winter at Wuqing (0.4 ng $m^{-3}$), which might be due to coal combustion for residential heating in the cold season.

The selected polycyclic aromatic hydrocarbons (PAH) were determined and shown in Figure 5-1c. The annual average concentration of the PAHs was 7.4±7.1 ng $m^{-3}$. These PAHs (indeno(1,2,3-cd) pyrene, benzo(g,h,i)perylene, coronene) with high molecular weight (MW>228) are common product of incomplete combustion and usually associated with vehicle emission particulate matter. The highest concentration was measured in winter and lowest in summer. The seasonal trend of these tracers indicted that the meteorological factors have a substantial impact on increased PAHs levels during the winter period. Such high-molecular-weight PAHs are stable enough to resist chemical reaction and evaporation (Schauer et al., 1996), and are preferentially accumulated on the fine particulate once emitted from motor vehicle exhaust when radiation inversion occurs in winter.

Levoglucosan, which is considered as a cellulose pyrolysis tracer (Simoneit et al., 1999), was observed higher in samples during fall and winter periods and lower level in summer with an annual average concentration of 452.7±337.6 ng $m^{-3}$ (Figure 5-1d). The measured concentrations of levoglucosan are much higher than reported value in some US sites (Lough et al., 2006). It is worthy to note that the concentration of levoglucosan observed in Zhongshan site increased dramatically with a much higher ratio of levoglucosan to OC (0.079) than that at other sites, which could be resulted from local biomass burning activity.

Meanwhile, cholesterol is thought as a tracer in meat charbroiling smoke (Rogge et al., 1991). As shown in Figure 5-1e, the cholesterol exhibited slightly higher level in winter than that in summer with an annual average concentration of 1.4±2.5 ng $m^{-3}$. Interestingly, the maximum value of 10.7 ng $m^{-3}$ was observed at Deyang site. Compared to other sites, such a sharp increase of cholesterol seemed to be impacted by local sources, i.e. meat cooking emissions.

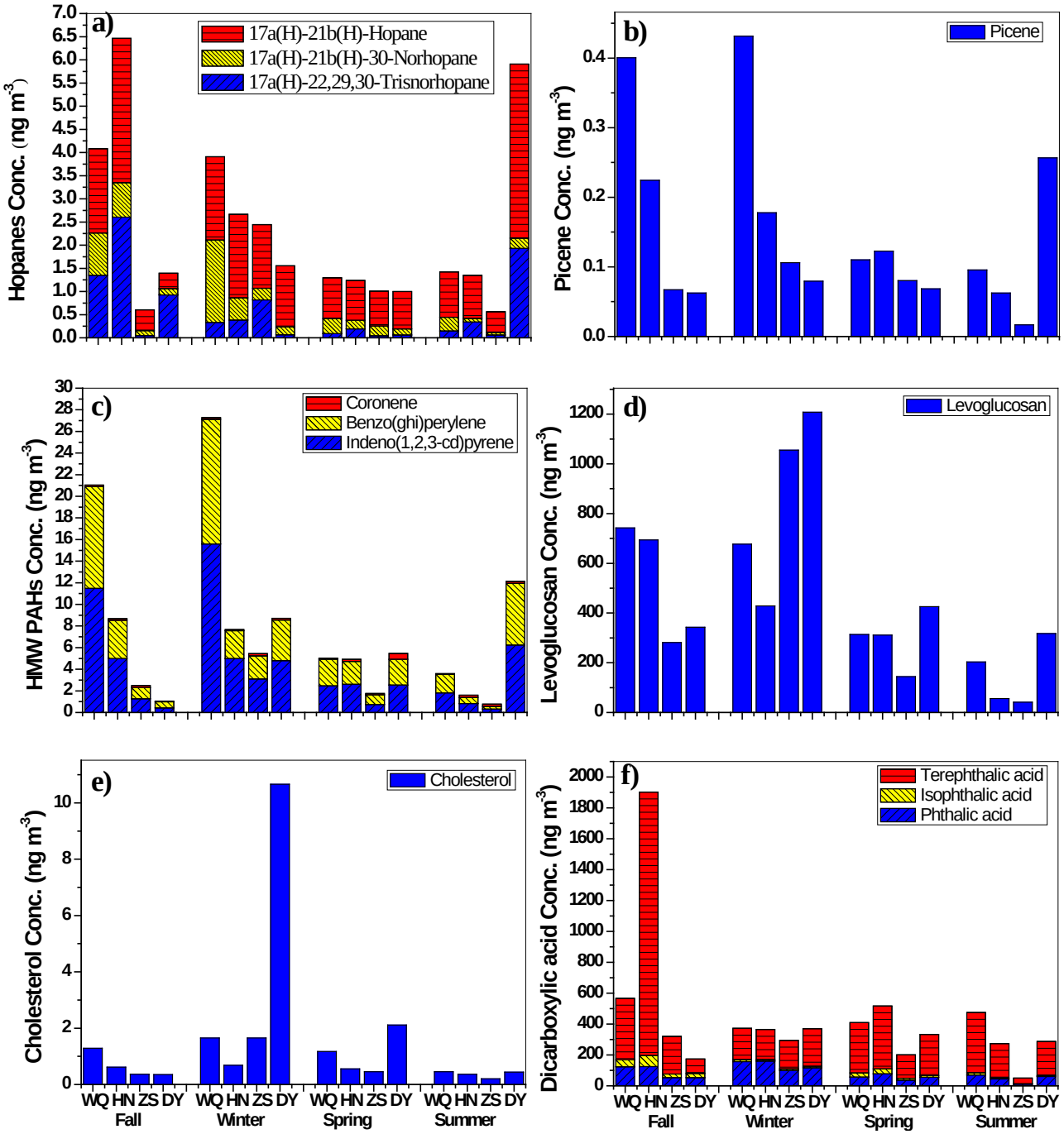


Figure 5-1 Seasonal variation of organic molecular marker at the sites in China Wuqing (WQ), Haining (HN), Zhongshan (ZS), Deyang (DY)

Aliphatic and aromatic diacids are commonly used as secondary organic aerosol tracers (Schauer et al., 2002; Zheng et al., 2002). The annual average concentration of collective these acids was 432.4±412.5 ng $m^{-3}$. The measured dicarboxylic acids (terephthalic acid, phthalic acid, isophthalic acid) had almost no clear seasonal trends and varied slightly across the sites except the samples at Zhongshan site during the fall period (Figure 5-1f). The similar treads in organic acids were observed in Baghdad, Iraq (Hamad, et al., 2015). It is possibly influenced by regional sources and also some meteorological factors.

### 5.3 Source apportionment of $PM_{2.5}$ OC

The primary source contributions to organic carbon in $PM_{2.5}$ was computed by molecular marker based CMB modeling method with the source profiles discussed previously as well as the concentration of fitting species determined from the ambient $PM_{2.5}$ samples (Schauer et al., 1996; Turpin et al., 2000).

The source apportionment model results for OC in $PM_{2.5}$ are shown in Figure 5-2. Analytical diagnostic values from MM-CMB model were listed in Table 5-1. The CMB results in this study are statistically significant with the average $R^2$, $CHI^2$ and the percent mass explained as 0.96, 1.01, and 84%, respectively. The other organic carbon category represents the difference between the measured total organic carbon concentration and the summed concentration of the primary source contributions quantified from the receptor model. Five sources are identified that contribute to the fine OC in this study, which varied in site and season. On an annual average, the vehicle emission, coal combustion, and biomass burning were found to be the most significant contributors to fine OC at these sites. Other identified primary sources include meat cooking and natural gas combustion.

The contribution to fine OC from these primary sources showed a distinct seasonal pattern. In spring, the vehicle emission was the largest contributor, which account for on average 47% of measured OC. The contribution to fine OC from this source were 5.03±1.65 μg $m^{-3}$, 2.21±0.69 μg $m^{-3}$ , 3.14±0.57 μg

$m^{-3}$, 9.56±2.76 μg $m^{-3}$ at Wuqing, Haining, Zhongshan, Deyang site, respectively. Vehicle emission dominated the sources contributing to the OC in summer, explaining on average 29% of OC. The lowest percentage of explained organic carbon to measured organic carbon was in summer at all sites (averaging 67%), possibly reflecting an increase in secondary organic aerosol formation in the hot season. A trend toward a higher contribution to the OC from biomass burning was found in fall, accounting for on average 41% of measured OC. Similar results were found at the urban sites in China and U.S. (Zheng et al., 2005; Zheng et al., 2007). Such dramatic increase of biomass aerosol contribution is possibly due to straw burning widely present around China at the time of the year. Interestingly, meat cooking showed a pronounced seasonal pattern, peaking in spring, with an average $PM_{2.5}$ OC contribution of 19% at these sites. In contrast, contributions from coal combustion increased greatly during cold months, accounting for 20% and 12% of OC in fall and winter, respectively.

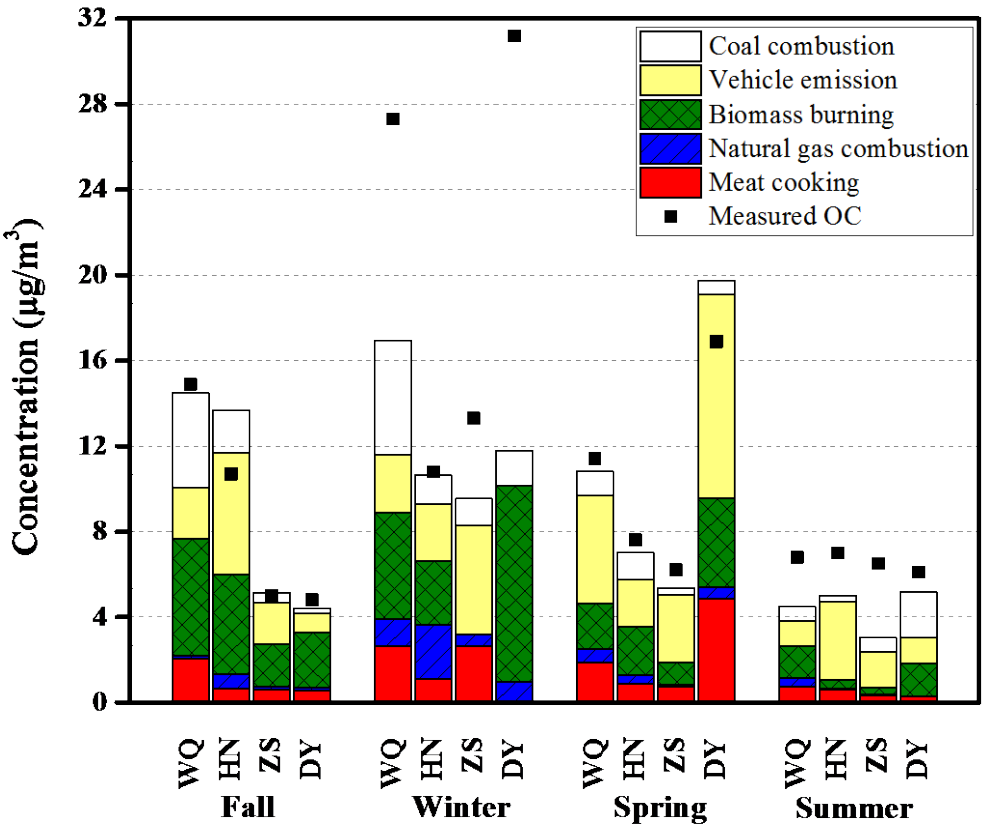


Figure 5-2 Seasonal variation in source apportionment of OC in $PM_{2.5}$ at the sites in China Wuqing (WQ), Haining (HN), Zhongshan (ZS), Deyang (DY)

**Table 5-1** Seasonal source contributions to OC in $PM_{2.5}$ at four sites of China (mean ± SD in μg $m^{-3}$)

| Site | Season | Meat cooking | Natural gas combustion | Biomass burning | Vehicle emission | Coal combustion | Sum of identified sources | Measured OC | $R^2$ | $CHI^2$ | %Mass explained |
|---|---|---|---|---|---|---|---|---|---|---|---|
| WQ | Fall | 2.05±0.58 | 0.12±0.76 | 5.49±1.76 | 2.40±0.59 | 4.42±0.60 | 14.5±2.1 | 14.9±3.0 | 0.97 | 0.80 | 97.2 |
| HN | Fall | 0.67±0.25 | 0.68±0.23 | 4.66±1.33 | 5.68±1.15 | 2.00±0.38 | 13.7±1.8 | 10.7±2.1 | 0.97 | 0.91 | 128.0 |
| ZS | Fall | 0.59±0.17 | 0.16±0.05 | 1.98±0.55 | 1.96±0.78 | 0.46±0.08 | 5.1±0.8 | 5.0±1.0 | 0.97 | 0.70 | 102.8 |
| DY | Fall | 0.56±0.16 | 0.14±0.04 | 2.58±0.82 | 0.91±0.15 | 0.23±0.07 | 4.4±1.1 | 4.8±1.0 | 0.97 | 0.98 | 91.6 |
| WQ | Winter | 2.64±0.74 | 1.25±0.54 | 5.01±1.60 | 2.69±0.56 | 5.35±0.82 | 16.9±3.1 | 27.3±3.5 | 0.97 | 0.81 | 62.1 |
| HN | Winter | 1.10±0.30 | 2.55±0.46 | 2.97±0.83 | 2.69±0.64 | 1.32±0.25 | 10.6±2.0 | 10.8±2.2 | 0.98 | 0.43 | 98.4 |
| ZS | Winter | 2.66±0.75 | 0.52±0.15 | ---[a] | 5.10±1.03 | 1.26±0.21 | 9.5±1.1 | 13.3±2.1 | 0.96 | 0.97 | 71.7 |
| DY | Winter | ---[a] | 0.97±0.23 | 9.17±2.87 | ---[a] | 1.64±0.25 | 11.8±3.0 | 31.2±4.2 | 0.96 | 0.85 | 37.8 |
| WQ | Spring | 1.88±0.53 | 0.63±0.15 | 2.13±0.60 | 5.03±1.65 | 1.15±0.21 | 10.8±1.4 | 11.4±2.3 | 0.95 | 1.47 | 94.8 |
| HN | Spring | 0.89±0.25 | 0.40±0.12 | 2.25±0.73 | 2.21±0.69 | 1.28±0.21 | 7.0±1.2 | 7.6±1.5 | 0.94 | 1.73 | 92.1 |
| ZS | Spring | 0.72±0.20 | 0.11±0.04 | 1.06±0.34 | 3.14±0.57 | 0.35±0.07 | 5.4±1.1 | 6.2±1.2 | 0.97 | 0.98 | 86.6 |
| DY | Spring | 4.85±1.37 | 0.55±0.12 | 4.14±1.15 | 9.56±2.76 | 0.65±0.14 | 19.8±2.6 | 16.9±3.4 | 0.95 | 1.59 | 116.9 |
| WQ | Summer | 0.73±0.21 | 0.40±0.09 | 1.52±0.48 | 1.16±0.22 | 0.69±0.15 | 4.5±0.6 | 6.8±1.4 | 0.95 | 1.34 | 66.2 |
| HN | Summer | 0.59±0.17 | 0.04±0.02 | 0.42±0.13 | 3.67±0.65 | 0.29±0.06 | 5.0±0.8 | 7.0±1.4 | 0.97 | 0.92 | 71.8 |
| ZS | Summer | 0.32±0.09 | 0.08±0.02 | 0.28±0.08 | 1.71±0.52 | 0.65±0.11 | 3.1±0.6 | 6.5±1.3 | 0.97 | 0.79 | 46.8 |
| DY | Summer | 0.28±0.15 | ---[a] | 1.53±0.45 | 1.23±0.34 | 2.13±0.26 | 5.2±1.0 | 6.1±1.2 | 0.97 | 0.85 | 84.5 |

[a] Source contribution to OC is insignificantly different from zero.

Model results revealed that the primary sources contributing to the $PM_{2.5}$ OC varied significantly by sites in this study. At Wuqing and Deyang site, the largest contributor to OC was biomass burning, explaining 23% and 30% of measured OC, respectively. While the vehicle emission had the most important impact on OC at Haining and Zhongshan site, with an annual average of 39% and 38% contributing to OC, respectively. When examining the CMB result, it is worthy to note that there is slight variation in vehicle emission, contributing between 2.82 and 3.56 ug $m^{-3}$ to OC across the sites.

### 5.4 Source apportionment of $PM_{2.5}$ mass

Since the ratio of the emissions of fine organic carbon to fine particle mass is known for each of the sources in the model, source contributions to fine particle mass concentrations also can be calculated. The following factors are used to convert fine organic carbon to fine particulate mass: 0.304 for vehicle emission, 0.336 for coal combustion, 0.588 for biomass burning, 0.849 for natural gas combustion, and 0.556 for meat cooking (Schauer et al., 1996; Schauer et al., 2000; Zheng et al., 2005). "Other mass" refers to the difference between $PM_{2.5}$ mass and the sum of identified sources. The other organic matter was calculated by multiplying the other organic carbon by 1.6. Figure 5-3 and Table 5-2 show the fine particle mass contributions from the primary sources plus the other organic matter as well as secondary sulfate, nitrate, and ammonium ion concentrations. The sum of identified primary sources and secondary aerosol formation accounted for between 47% and 60% of the measured $PM_{2.5}$ mass during different seasons. The major contributors to $PM_{2.5}$ mass in this study were calculated as secondary sulfate (16.1±9.3 μg $m^{-3}$), secondary nitrate (11.1±8.6 μg $m^{-3}$), vehicle emission (10.1±7.7 μg $m^{-3}$), secondary ammonium (5.0±4.0 μg $m^{-3}$), biomass burning (4.8±4.1 μg $m^{-3}$), coal combustion (4.4±4.3 μg $m^{-3}$), meat cooking (2.3±2.2 μg $m^{-3}$), other organic matter (4.5±8.2 μg $m^{-3}$), and natural gas combustion (0.6±0.7 μg $m^{-3}$) on annual average.

From the source apportionment results, the secondary inorganic ions including sulfate, nitrate and ammonium were found the major components in $PM_{2.5}$. Meanwhile, the other organic matter varied greatly between the seasons, especially contributing average 11% of the sum of identified sources in summer. A high portion of “other OM” in summer is mainly associated with secondary organic aerosol formed when volatile organic precursor compound and oxidant species exists at warm months of the year. However, we note that it may also have other small sources of primary organics, which are not included in the model such as industrial sources and road dust.

The highest percentage of identified source contribution to $PM_{2.5}$ was found at Zhongshan site, accounting for 63% of total mass, while the lowest at Deyang site explained only 52% of the mass. Interestingly, the secondary sulfate, nitrate, and ammonium have minor variation across the sites during wintertime, with relative standard deviation of 16.3-33.5%, confirming the influences of regional emission sources on these sites.

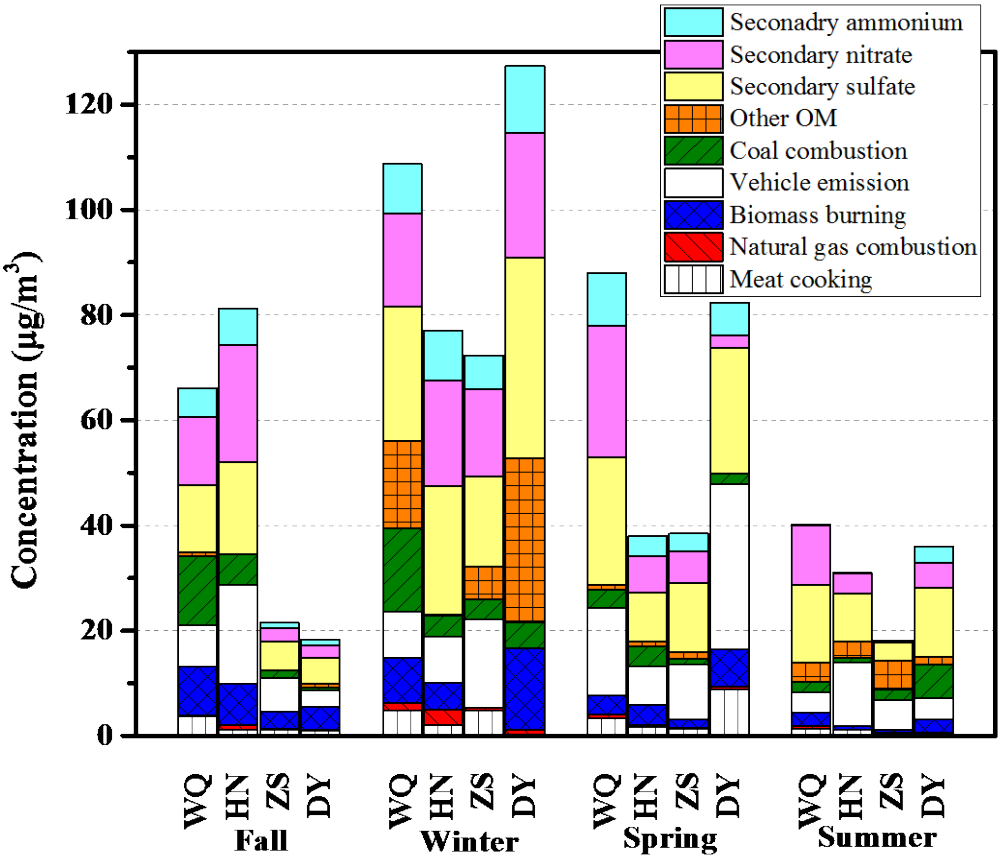


Figure 5-3 Source contributions to $PM_{2.5}$ mass at the sites in China

Wuqing (WQ), Haining (HN), Zhongshan (ZS), Deyang (DY)

**Table 5-2** Seasonal source apportionments of $PM_{2.5}$ mass concentration at four sites of China (μg $m^{-3}$)

| Site | Season | Meat cooking | Natural gas combustion | Biomass burning | Vehicle emission | Coal combustion | Other organic matter | Secondary sulfate | Secondary nitrate | Secondary ammonium | %Mass explain |
|---|---|---|---|---|---|---|---|---|---|---|---|
| WQ | Fall | 3.69 | 0.14 | 9.34 | 7.89 | 13.15 | 0.64 | 12.83 | 12.86 | 5.57 | 58.2 |
| HN | Fall | 1.21 | 0.80 | 7.93 | 18.68 | 5.95 | 0.00 | 17.57 | 22.10 | 7.05 | 51.4 |
| ZS | Fall | 1.06 | 0.19 | 3.37 | 6.54 | 1.37 | 0.00 | 5.57 | 2.47 | 1.04 | 71.5 |
| DY | Fall | 1.01 | 0.16 | 4.39 | 2.99 | 0.68 | 0.61 | 5.06 | 2.32 | 1.01 | 60.7 |
| WQ | Winter | 4.75 | 1.47 | 8.52 | 8.85 | 15.92 | 16.64 | 25.55 | 17.62 | 9.52 | 65.2 |
| HN | Winter | 1.98 | 3.00 | 5.05 | 8.85 | 3.93 | 0.27 | 24.46 | 19.98 | 9.55 | 60.8 |
| ZS | Winter | 4.78 | 0.61 | ---[a] | 16.78 | 3.75 | 6.34 | 16.97 | 16.60 | 6.47 | 62.0 |
| DY | Winter | ---[a] | 1.14 | 15.60 | ---[a] | 4.88 | 31.09 | 38.22 | 23.77 | 12.61 | 49.6 |
| WQ | Spring | 3.38 | 0.74 | 3.62 | 16.55 | 3.42 | 0.94 | 24.27 | 25.06 | 9.99 | 59.1 |
| HN | Spring | 1.60 | 0.47 | 3.83 | 7.27 | 3.81 | 0.91 | 9.41 | 6.89 | 3.75 | 55.0 |
| ZS | Spring | 1.29 | 0.13 | 1.80 | 10.33 | 1.04 | 1.30 | 13.21 | 5.97 | 3.39 | 65.8 |
| DY | Spring | 8.72 | 0.65 | 7.04 | 31.45 | 1.93 | 0.00 | 23.99 | 2.33 | 6.25 | 60.7 |
| WQ | Summer | 1.31 | 0.47 | 2.59 | 3.82 | 2.05 | 3.68 | 14.67 | 11.39 | 0.29 | 37.3 |
| HN | Summer | 1.06 | 0.05 | 0.71 | 12.07 | 0.86 | 3.17 | 9.11 | 3.77 | 0.18 | 47.9 |
| ZS | Summer | 0.58 | 0.09 | 0.48 | 5.63 | 1.93 | 5.52 | 3.57 | 0.15 | 0.09 | 57.3 |
| DY | Summer | 0.50 | ---[a] | 2.60 | 4.05 | 6.34 | 1.47 | 13.24 | 4.65 | 3.12 | 44.0 |

[a] Contribution to $PM_{2.5}$ mass is insignificantly different from zero.

Overall, the annual average source contribution to $PM_{2.5}$ mass at four sites of China was shown in Figure 5-4. At Wuqing and Haining site, the major contributors to $PM_{2.5}$ mass were secondary sulfate (26-27%), secondary nitrate (22-23%) and vehicle emission (12-21%). In contrast, vehicle emission (26%) and secondary sulfate (26%) have the highest impact on $PM_{2.5}$ mass at Zhongshan site. The secondary sulfate was found to the highest contributor, accounting for 30% of $PM_{2.5}$ mass at Deyang site, followed by vehicle emission (15%) and secondary nitrate (12%). The secondary ammonium showed little change across the sites, contributing 7-9% of the $PM_{2.5}$ mass. Meanwhile, biomass burning accounted for 4-12% of fine particles, and it has a higher impact at Deyang compared to other sites. The coal combustion has relatively higher contributing to $PM_{2.5}$ mass at Wuqing site (12%), whereas the other sites were found to be around 6%. It is not surprising that the coal combustion is widely used for residential heating at Wuqing during the cold months. However, there is no central heating in winter at southern cities of China. We note that the present results were confirmed by the findings of Andersson et al. using dual carbon isotope constrained ($\Delta^{14}C$ and $\delta^{13}C$) source apportionment technology during the same study period (Andersson et al., 2015). It was found that higher coal combustion is contributing to EC in NCP region and more liquid fossil in YRD and PRD region. In addition, small amounts of $PM_{2.5}$ mass are contributed by meat cooking (2-5%), natural gas combustion (1-2%), and other OM (2-13%).

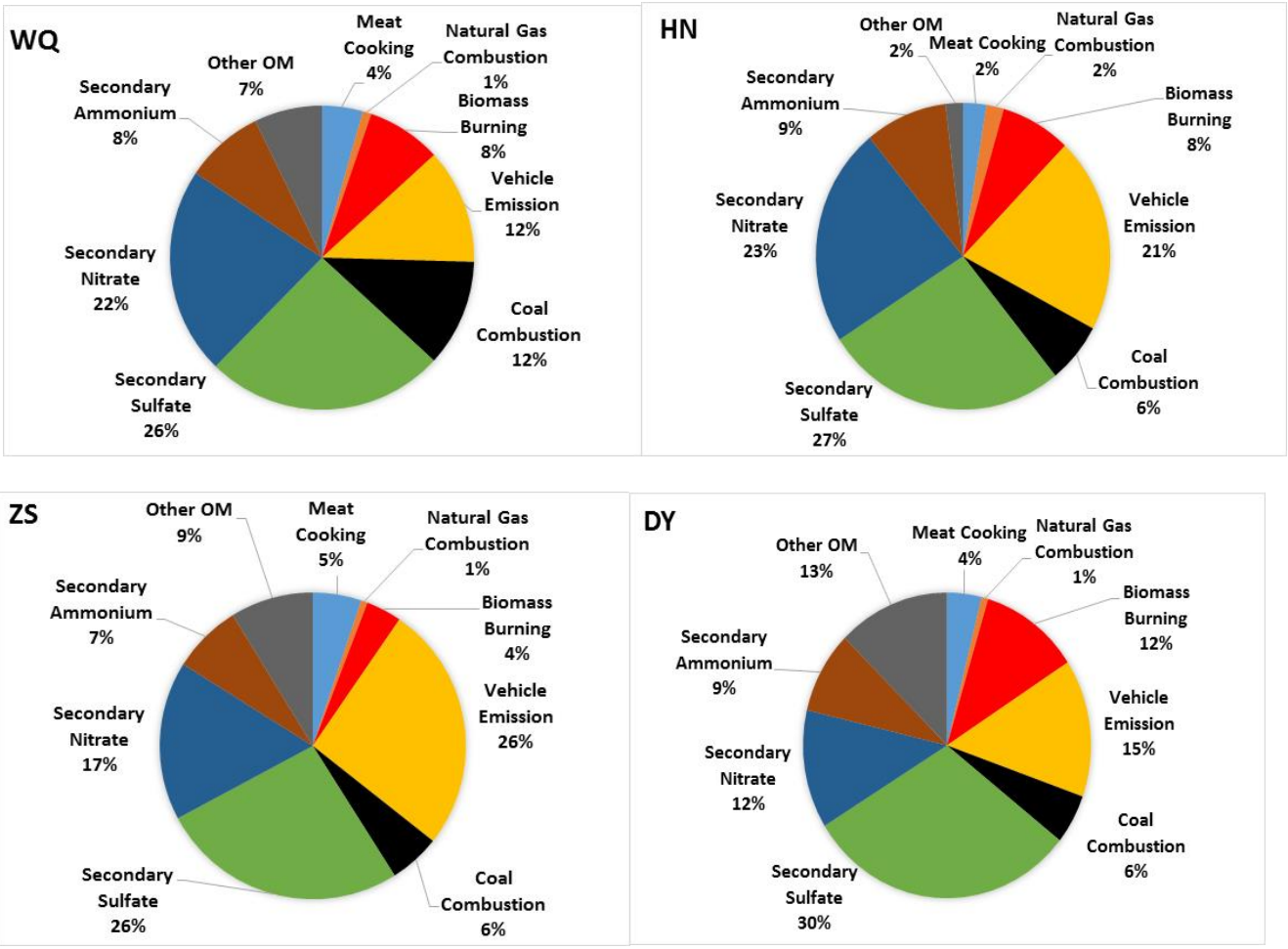


Figure 5-4 Annual average source contribution to $PM_{2.5}$ mass at four sites in China

## 5.5 Summary

To investigate the organic constituents of ambient fine PM and quantify the source contributions to $PM_{2.5}$ mass, a sampling campaign was conducted at four satellite city sites in China over a one-year period of 2012-2013. A molecular marker-chemical mass balance (CMB) receptor model was applied to apportion the seasonal source contributions to OC and $PM_{2.5}$ mass at these sites. The CMB results revealed that the major primary sources of $PM_{2.5}$ carbonaceous aerosol are vehicle emission, biomass burning, coal combustion, meat cooking and natural gas combustion. These primary sources collectively accounted for 84±24% of measured OC with a relative lower contribution in summer

(67%), which could be associated with secondary formation processes. The sum of identified primary sources and secondary aerosol formation accounted for between 47% and 60% of the measured $PM_{2.5}$ mass on average. The major contributors to $PM_{2.5}$ mass were secondary sulfate (26-30%), secondary nitrate (12-23%), vehicle emission (12-26%), coal combustion (6-12%), secondary ammonium (7-9%), biomass burning (4-12%), meat cooking (2-5%), natural gas combustion (1-2%), and other OM (2-13%) on annual average at these sites. Source contribution showed distinct seasonality with higher contribution from biomass burning in fall and more coal combustion emission in winter. The secondary ammonium has minor variation across the sites, especially during wintertime, which was possibly due to the impact from regional emission sources on these sites. Local source contributors to the fine particulate matter at these sites were observed, including the highest vehicle emission at Zhongshan site (26%) and highest contribution from biomass burning at Deyang site (12%). Therefore, the source apportionment results based on molecular marker receptor model in this study is helpful for developing both regional and local mitigation strategies for fine particulate matter in the various urban area of China.

# Chapter 6 Conclusions and Recommendations

## 6.1 Conclusions

The chemical composition of airborne fine aerosol $PM_{2.5}$ collected at four satellite city sites (Wuqing, Haining, Zhongshan, Deyang) in China over a one-year period of 2012-2013 were investigated in this study. The influence of regional transport on the seasonal variation of $PM_{2.5}$ across the sites was studied by using back trajectories HYSPLIT model. The molecular marker based CMB model was applied to estimate source contributions to organic carbon (OC) and $PM_{2.5}$ mass. The more details are summarized herein.

The annual average $PM_{2.5}$ mass concentrations ranged from 60.5 to 148.9 μg $m^{-3}$, which is much higher than the National Ambient Air Quality Standards (NAAQS) of China for $PM_{2.5}$ (35 μg $m^{-3}$ annual average). The Wuqing site had the highest concentration of aerosol $PM_{2.5}$, followed by Deyang and Haining, while Zhongshan site was found being the lowest. The $PM_{2.5}$ at Wuqing site is characterized by higher water-soluble inorganic ions and lower OM composition. In contrast, Zhongshan site showed a higher relative abundance of OM particles whereas lower water-soluble ions.

The water-soluble ions were dominated by three ionic species ($SO_4^{2-}$, $NO_3^-$, $NH_4^+$) accounting for 33-41% of the $PM_{2.5}$ mass. In general, water-soluble ions exhibited a clear seasonal pattern with the highest concentration in winter while lower in summer. Additionally, the total carbonaceous particle matter approximately comprised 16-23% of the $PM_{2.5}$ mass.

The fine aerosols at four sites were characterized by acidic in nature based on ion balance calculations. It means the neutralization of sulfate and nitrate in aerosol was not complete. Under the ammonium-poor condition, the positive correlations between nss-$SO_4^{2-}$ and $NH_4^+$ ($R=0.92-0.98$) at a very significant level ($P<0.001$) revealed the sulfate aerosol primarily existed in the form of $(NH_4)_2SO_4$ in the atmosphere at these sites.

The aerosol chemical composition combined with back trajectory analysis confirmed that both long-range transport and local emissions have important impact on ions and carbonaceous particles in the aerosol at these sites. The majority of the air masses during summertime reaching these sites were from western Pacific Ocean passing over Yangtze River Delta (YRD), Pearl River Delta (PRD) regions, whereas at Deyang site the air mass originated from southern mainland coupling with local Sichuan Basin (SB) emissions and long-range transport from South Asia.

The dust originating in the Mongolia moved southeastward and mixed with air masses passing over North China Plain (NCP), and finally arrived at Wuqing site during wintertime. The fine aerosol chemical data in winter is characterized by high level of $Ca^{2+}$ (1.3 μg $m^{-3}$), $Mg^{2+}$ (0.2 μg $m^{-3}$), $NO_3^-$ (25.2 μg $m^{-3}$), $SO_4^{2-}$ (40.9 μg $m^{-3}$), OC (27.3 μg $m^{-3}$), and $K^+$ (7.2 μg $m^{-3}$), suggesting the polluted air masses was mixed with fossil fuel combustion and continental dust via long-range transport.

The characteristic chemical species ratios ($SO_4^{2-}/PM_{2.5}$, $NO_3^-$/PM2.5) in $PM_{2.5}$ at these sites implied relatively higher coal combustion emission in NCP region, whereas a relatively greater contribution from traffic emissions at Haining and Zhongshan sites during the winter.

The principal component analysis (PCA) technique was applied with major aerosol data to identify the main contributions of processes and emission sources of water-soluble ions. PCA result indicated that major sources of ions are vehicular emissions, coal/biomass combustion, industry source, as well as soil dust.

A molecular marker-chemical mass balance (CMB) receptor model was applied to apportion the seasonal source contributions to OC and $PM_{2.5}$ mass at these sites. The CMB results revealed that the major primary sources of $PM_{2.5}$ carbonaceous aerosol are vehicle emission, biomass burning, coal combustion, meat cooking and natural gas combustion. These primary sources collectively accounted for 84±24% of measured OC with a relative lower contribution in summer (67%), which could be associated with secondary formation processes.

The sum of identified primary sources and secondary aerosol formation accounted for between 47% and 60% of the measured $PM_{2.5}$ mass on average. The major contributors to $PM_{2.5}$ mass were secondary sulfate (26-30%), vehicle emission (12-26%), secondary nitrate (12-23%), secondary ammonium (7-9%), coal combustion (6-12%), biomass burning (4-12%), meat cooking (2-5%), natural gas combustion (1-2%), and other OM (2-13%) on annual average at these sites.

Source contribution showed distinct seasonality with higher contribution from biomass burning in fall and more coal combustion emission in winter. Local source contributors to the fine particulate matter at these sites were observed, including the highest vehicle emission at Zhongshan site (26%) and highest contribution from biomass burning at Deyang site (12%).

The source apportionment results based on molecular marker receptor model in this study is helpful for developing both regional and local mitigation strategies to decrease $PM_{2.5}$ concentrations in the various urban area of China.

This work has contributed to improvement in understanding chemical nature of aerosol fine particulate matter. Meanwhile, this work has advanced future source apportionment study to distinguish primary and secondary aerosol sources and evaluate the impacts of local and regional emissions on air quality.

### 6.2 Recommendations

Based on the experimental and model results in this thesis, several recommendations for the future work are proposed below.

More studies on local source profiles for these sites in China will give a better understanding of sources of fine aerosol and improve the accuracy of source apportionment model result.

It would be valuable to collecting more detailed meteorological data at these sites during sampling campaign thereby study some major factors influencing the spatiotemporal variability of $PM_{2.5}$ aerosol chemical compositions.

It would be interesting to compare the source apportionment result using other techniques such as positive matrix factorization (PMF), UNMIX model, carbon isotope analysis, and therefore provide more reliable source apportionment result.

Because the CMB model applied in this study was only to apportion the primary sources of fine aerosol OC, further studies focused on secondary organic aerosol will allow us to fill the gaps between identified OC and measured OC in $PM_{2.5}$.

## References


Aggarwal, S. G., Kawamura, K. (2009). Carbonaceous and inorganic composition in long-range transported aerosols over northern Japan: Implication for aging of water-soluble organic fraction *Atmos. Environ.*, 43, 2532-2540.

Andersson, A., Deng, J., Du, K., Zheng, M., Yan, C., Sköld, M., Gustafsson, Ö. (2015). Regionally-varying combustion sources of the January 2013 severe haze events over China, *Environ. Sci. Technol.*, 49, 2038-2043.

Andreae, M. O., Andreae, T. W., Annegarn, H., Beer, J., Cachier, H., Canut, P., Elbert, W., Maenhaut, W., Salma, I., Wienhold, F. G., Zenker, T. (1998). Airborne studies of aerosol emissions from savanna fires in southern Africa: aerosol chemical composition. *J. Geophys. Res.*, 103, (D24), 32119-32128.

Bauer, S. E., Koch, D., Unger, N., Metzger, S. M., Shindell, D. T., Streets, D. G. (2007). Nitrate aerosols today and in 2030: a global simulation including aerosols and tropospheric ozone. *Atmos. Chem. Phys.*, 7, 5043-5059.

Brimblecombe, P. (1996). Air Composition & Chemistry, Cambridge University Press, Cambridge.

Cao, J. J., Lee, S. C., Ho, K. F., Zhang, X. Y., Zou, S. C., Fung, K. K., Chow, J. C., Watson, J. G. (2003). Characteristics of carbonaceous aerosol in Pearl River Delta region, China during 2001 winter period. *Atmos. Environ.*, 37, 1451-1460.

Cao, J. J., Shen, Z. X., Chow, J. C., Watson, J. G., Lee, S. C., Tie, X. X., Ho, K. F., Wang, G. H., Han, Y. M. (2012). Winter and summer $PM_{2.5}$ chemical compositions in fourteen Chinese cities. *J. Air Waste Manage. Assoc.*, 62, 1214-1226.

Cao, J. J., Chow, J. C., Lee, Frank S. C., Watson, J. G. (2013). Evolution of $PM_{2.5}$ Measurements and Standards in the U.S. and Future Perspectives for China. *Aerosol and Air Quality Research*, 13, 1197-1211.

Cao, G., Zhang, X., Zheng, F. (2006). Inventory of black carbon and organic carbon emissions from China. *Atmos. Environ.*, 40, 6516-6527.

Charlson, R. J., S. E. Schwartz, J. M. Hales, R. D. Cess, Coakley, J. A., Hansen, J. E., Hofmann, D. J. (1992). Climate forcing by anthropogenic aerosols. *Science*, 255, 423-430.

Cheung, K., Daher, N., Kam, W., Shafer, M. M., Ning, Z., Schauer, J. J. (2011). Spatial and temporal variation of chemical composition and mass closure of ambient coarse particulate matter ($PM_{10-2.5}$) in the Los Angeles area. *Atmos. Environ*., 45, 2651-62.

Chin, M., Ginoux, P., Kinne, S., Torres, O., Holben, B. N., Duncan, B. N., Martin, R. V., Logan, J. A., Higurashi, A., Nakajima, T. (2002). Tropospheric aerosol optical thickness from the GOCART model and comparisons with satellite and sunphotometer measurements. *J. Atmos. Sci.*, 59, 461-483.

Chow, J. C., Watson, J. G., Fujita, E. M., Lu, Z., Lawson, D. R. (1994). Temporal and spatial variations of $PM_{2.5}$ and $PM_{10}$ aerosol in the Southern California air quality study. *Atmos. Environ*. 28, 2061-2080.

Chow, J. C. (1995). Critical Review: Measurement Methods to Determine Compliance with Ambient Air Quality Standards for Suspended Particles. *J. Air Waste Manage. Assoc*. 45: 320–382.

Chow, J. C., Chen, L. W. A., Watson, J. G., Lowenthal, D. H., Magliano, K. A., Turkiewicz, K., Lehrman, D. E. (2006). $PM_{2.5}$ chemical composition and spatiotemporal variability during the California regional $PM_{10}$/$PM_{2.5}$ air quality study (CRPAQS). *Journal of Geophysical Research*, 111, D10S04.

Draxler, R. R., Hess, G. D. (1998). An overview of the HYSPLIT 4 modelling system for trajectories, dispersion, and deposition. *Aust. Meteorol. Mag.* 47, 295-308.

Du, H. H., Kong, L. D., Cheng, T. T., Chen, J. M., Du, J. F., Li, L., Xia, X. G., Leng, C. P., Huang, G. H. (2011). Insights into summertime haze pollution events over Shanghai based on online water-soluble ionic composition of aerosols. *Atmos. Environ.*, 45, 5131-5137.

Duan, F. K., He, K. B., Ma, Y. L., Yang, F. M., Yu, X. C., Cadle, S. H., Chan, T., Mulawa P. A. (2006). Concentration and chemical characteristics of $PM_{2.5}$ in Beijing, China: 2001-2002. *Sci. Total Environ.*, 355, 264-275.

Dunker, A. M., Yarwood, G., Ortmann, J. P., Wilson, G. M. (2002). Comparison of source apportionment and source sensitivity of ozone in a three-dimensional air quality model. *Environ. Sci. Technol.*, 36, 2953-2964.

Eder, B., Bash, J., Foley, K., Pleim, J. (2014). Incorporating principal component analysis into air quality model evaluation. *Atmos. Environ.*, 82, 307-315.

Fine, P. M., Cass, G. R., Simoneit, B.R.T. (2004). Chemical Characterization of Fine Particle Emissions from the Fireplace Combustion of Wood Types Grown in the Midwestern and Western United States. *Environ. Eng. Sci.*, 21, 387-409.

Hamad, S. H., Schauer, J. J., Heo, J., Kadhim, A. K. H. (2015). Source apportionment of $PM_{2.5}$ carbonaceous aerosol in Baghdad, Iraq. *Atmos. Res.*, 156, 80-90.

Harrison, R. M., van Grieken, R. E. (1998). Atmospheric Particles, John Wiley and Sons.

Harrison, R. M., Yin, J. (2000). Particulate matter in the atmosphere: which particle properties are important for its effects on health? *Sci. Total Environ.*, 249, 85-101.

He, K. B., Yang, F. M., Ma, Y. L., Zhang, Q., Yao, X. H., Chan, C. K., Cadle, S. H., Chan, T., Mulawa, P. A. (2001). The characteristics of $PM_{2.5}$ in Beijing, China. *Atmos. Environ.*, 35, 4959-4970.

Hennigan, C. J., Izumi, J., Sullivan, A. P., Weber, R. J., Nenes, A. (2015). A critical evaluation of proxy methods used to estimate the acidity of atmospheric particles. *Atmos. Chem. Phys.*, 15, 2775- 2790.

Ho, K. F., Lee, S. C., Chan, C. K., Yu, J., Chow, J. C., Yao, X. H. (2003). Characterization of chemical species in $PM_{2.5}$ and $PM_{10}$ aerosols in Hong Kong. *Atmos. Environ.*, 37, 31-39.

Hopke, P. K. (1991). An introduction to receptor modelling. Chemometrics and Intelligent Laboratory Systems 10, 21-43.

Hu, G., Zhang, Y. M., Sun, J. Y., Zhang, L. M., Shen, X. J., Lin, W. L., Yang, Y. (2014). Variability, formation and acidity of water-soluble ions in $PM_{2.5}$ in Beijing based on the semi-continuous observations. *Atmos. Res.*, 145-146, 1-11.

Hu, M., Ling, Y. H., Zhang, Y. H., Wang, M., Kim, Y. P., Moon, K. C. (2002). Seasonal variation of ionic species in fine particles at Qingdao, China. *Atmos. Environ.*, 36, 5853-5859.

Hu, M., Wu, Z. J., Slanina, J., Lin, P., Liu, S., Zeng, L. M. (2008). Acidic gases, ammonia and water-soluble ions in $PM_{2.5}$ at a coastal site in the Pearl River Delta, China. *Atmos. Environ.*, 42, 6310-6320.

Hueglin, C., Gehrig, R., Baltensperger, U., Gysel, M., Monn, C., Vonmont, H. (2005). Chemical characterisation of $PM_{2.5}$, $PM_{10}$ and coarse particles at urban, near-city and rural sites in Switzerland. *Atmo. Environ.*, 39, 637-651.

IMPROVE. (2000). Spatial and seasonal patterns and temporal variability of haze and its constituents in the United States. Report III.Available from: http://vista.cira.colostate.edu/improve/Publications /Reports/2000/2000.htm.

Jacobson, M. C., Hansson, H. C., Noone, K. J., Charlson, R. J. (2000). Organic atmospheric aerosols: Review and state of the science. *Rev. Geophys.*, 38, 267-294.

Jaeckels, J. M., Bae, M. S., Schauer, J. J. (2007). Positive Matrix Factorization (PMF) analysis of molecular marker measurements to quantify the sources of organic aerosols. *Environ. Sci. Technol.*, 41 (16), 5763-5769.

Jaoui, M., Kamens, R. M. (2003). Photolysis Study of Gas Phase Pinonaldehyde in the Presence of

Natural Sunlight. *Atmos. Environ.*, 37: 1835-1851.

Kallos, G., Astitha, M., Katsafados, P., Spyrou, C. (2007). Long-range transport of anthropogenically and naturally produced particulate matter in the Mediterranean and North Atlantic: current state of knowledge. *Journal of Applied Meteorology and Climatology*, 46, 1230-1251.

Kanakidou, M., Seinfeld, J. H. and Pandis S. N. (2005). Organic Aerosol and Global Climate Modelling: a Review. *Atmos. Chem. Phys.*, 5: 1053-1123.

Kavouras, I. G., Mihalopoulos, N., Stephanou, E. G. (1999). Secondary Organic Aerosol Formation vs Primary Organic Aerosol Emission: in situ Evidence for the Chemical Coupling Between Monoterpene Acidic Photooxidation Products and New Particle Formation over Forests. *Environ. Sci. Technol.*, 33, 1028-1037.

Kleeman, M. J., Cass, G. R. (2001). A 3D Eulerian source-oriented model for an externally mixed aerosol. *Environ. Sci. Technol.*, 35, 4834-4848.

Kleindienst, T. E., Edney, E. O., Lewandowski, M., Offenberg J. H., Jaoui, M. (2006). Secondary Organic Carbon and Aerosol Yields from the Irradiations of Isoprene and α-Pinene in the Presence of NOx and SO2. *Environ. Sci. Technol.*, 40: 3807-3812.

Khoder, M. I., Hassan, S. K. (2008). Weekday/weekend differences in ambient aerosol level and chemical characteristics of water-soluble components in the city centre. *Atmos. Environ.*, 42, 7483-7493.

Kim, K. H., Kabir, E., Kabir, S. (2015). A review on the human health impact of airborne particulate matter. *Environ. Int.*, 74, 136-143.

Kiss, G., Gelencser, A., Hoffer, A., Krivacsy, Z., Meszaros, E., Molnar, A., and Varga, B. (2000). Chemical characterisation of water soluble organic compounds in tropospheric fine aerosol, *Proc. Conf. on Nucleation and Atmospheric Aerosols*, 761-764.

Kundu, S., Kawamura, K., Andreae, T. W., Hoffer, A., Andreae, M. O. (2010). Diurnal variation in the water-soluble inorganic ions, organic carbon and isotopic compositions of total carbon and nitrogen in biomass burning aerosols from the LBA-SMOCC campaign in Rondônia, Brazil. *Aerosol Sci.*, 41, 118-133.

Lestaria, P., Oskouie, A. K., Noll, K. E. (2003). Size distribution and dry deposition ofparticulate mass, sulfate and nitrate in an urban area. *Atmos. Environ.,* 37, 2507-2516.

Li, J., Posfai, M., Hobbs, P. V., Buseck, P. R. (2003). Individual aerosol particles from biomass burning in southern Africa: 2 Compositions and aging of inorganic particles. *J. Geophys. Res.*, 108 (D13), doi: http://dx.doi.org//10.1029/2002JD002310.

Lin, Y. C., Cheng, M. T., Lin, W. H., Lan, Y. Y., Tsuang, B. J. (2010). Causes of the elevated nitrate aerosol levels during episodic days in Taichung urban area, Taiwan. *Atmos. Environ.*, 44, 1632-1640.

Lough, G. C., Schauer, J. J., Lawson, D. R. (2006). Day-of-Week Trends in Carbonaceous Aerosol Composition in the Urban Atmosphere. *Atmos. Environ.*, 40, 4137-4149.

Lough, G. C., Christensen, C. G., Schauer, J. J., Tortorelli, J., Mani, E., Lawson, D. R. (2007). Development of Molecular Marker Source Profiles for Emissions from On-Road Gasoline and Diesel Vehicle Fleets. *J. Air Waste Manage. Assoc.*, 57, 1190-1199.

Lu, W. Z., He, H. D., Dong, L. Y. (2011). Performance assessment of air quality monitoring networks using principal component analysis and cluster analysis. *Build Environ.,* 46, 577-583.

Manchester-Neesvig, J. B., Schauer, J. J., Cass, G. R. (2003). The Distribution of Particle-Phase Organic Compounds in the Atmosphere and Their Use for Source Apportionment during the Southern California Children's Health Study. *J. Air Waste Manage. Assoc.*, 53, 1065-1079.

McCulloch, A., Aucott, M. L., Benkovitz, C. M., Graedel, T. E., Kleiman, G., Midgley, P. M., Li, Y. (1999). Global emissions of hydrogen chloride and chloromethane from coal combustion,

incineration and industrial activities: Reactive chlorine emissions inventory. *J. Geophys. Res.*, 104 (D7), 8391-8403.

Meng, Z. Y., Zhang, R. J., Lin, W. L., Jia, X. F., Yu, X. M., Yu, X. L., Wang, G. H. (2014). Seasonal variation of ammonia and ammonium aerosol at a background station in the Yangtze River Delta region, China. *Aerosol Air Qual. Res.*, 14, 756-766.

Meng, Z., Seinfeld, J. H. (1994). On the source of the submicrometer droplet mode of urban and regional aerosols. *Aerosol. Sci. Technol.* 20, 253-265.

Mohapatra, K., Biswal, S. K. (2014). Effect of particulate matter (PM) on plants, climate, ecosystem and human health. *Int. J. Adv. Technol. Eng.Sci.*, 2, 118-129.

Morales, J. A., Pirela, D., de Nava, M. G., de Borrego, B. S., Velásquez, H., Durán, J. (1998). Inorganic water soluble ions in atmospheric particles over Maracaibo Lake Basin in the western region of Venezuela. *Atmos. Res.*, 46, 307-320.

Nolte, C. G., Schauer, J. J., Cass, G. R., Simoneit, B. R. T. (2002). Trimethylsilyl derivatives of organic compounds in source samples and in atmospheric fine particulate matter. *Environ. Sci. Technol.*, 36, 4273-4281.

Odum, J. R., Jungkamp, T. P. W., Griffin, R. J., Flagan, R. C., Seinfeld, J. H. (1997). The Atmospheric Aerosol-Forming Potential of Whole Gasoline Vapor. *Science*, 276, 96-99.

Oros, D., Simoneit, B. R. T. (2000). Identification and emission rates of molecular tracers in coal smoke particulate matter. *Fuel*, 79, 515-536.

Pandis, S. N., Seinfeld, J. H., Pilinis, C. (1990). The Smog-Fog-Smog cycle and acid deposition. *J. Geophys. Res.* 95 (D11), 18489-18500.

Paode, R. D., Shahin, U. M., Sivadechathep, J., Holsen, T. M., Franek, W. J. (1999). Source Apportionment of Dry Deposited and Airborne Coarse Particles Collected in the Chicago Area. *Aerosol Sci. Technol.*, 31, 473-486.

Paraskevopoulou, D., Liakakou, E., Gerasopoulos, E., Mihalopoulos, N. (2015). Sources of atmospheric aerosol from long-term measurements (5 years) of chemical composition in Athens, Greece. *Sci. Total Environ.*, 527-528, 165-178.

Pathak, R. K., Wu, W. S., Wang, T. (2009). Summertime $PM_{2.5}$ ionic species in four major cities of China: nitrate formation in an ammonia-deficient atmosphere. *Atmos. Chem. Phys.*, 9, 1711-1722.

Pekney, N. J., Davidson, C. I., Robinson, A., Zhou, L. M., Hopke, P. K., Eatough, D. J., Rogge, W. F. (2006). Major Source Categories for PM2.5 in Pittsburgh Using PMF and UNMIX. *Aerosol Sci. Technol.* 40, 910-924.

Pope, III C. A., Burnett, R. T., Thun, M. J. (2002). Lung cancer, cardiopulmonary mortality and long-term exposure to fine particulate air pollution. *J. Amer. Med. Assoc.*, 287, 1132-1141.

Pope, C. A., Dockery, D. W. (2006). Health effects of fine particulate air pollution: lines that connect. *J. Air Waste Manage. Assoc.*, 56, 709-742.

Putaud, J. P., Dingenen, R. V., Dell'Acqua, A., Raes, F., Matta, E., Decesari, S., Facchini, M. C., Fuzzi, S. (2004). Size-segregated aerosol mass closure and chemical composition in Monte Cimone (I) during MINATROC. *Atmos. Chem. Phys.*, 4, 889-902.

Raizenne, M., Neas, L. M.; Damokosh, A. L., Dockery, D. W., Spen-gler, J. D., Koutrakis, P., Ware, J. H., Speizer, F. E. (1996). Health effects of acid aerosols on North American children: pulmonary function. *Environ. Health Perspect.*, 104, 506-514.

Roberts, G. C., Andreae, M. O., Zhou, J., Artaxo, P. (2001). Cloud condensation nuclei in the Amazon Basin: “Marine” conditions over a continent. *Geophys. Res. Lett.*, 28(14), 2807-2810.

Robinson, A. L., Subramanian, R., Donahue, N. M., Bernardo-Bricker, A., Rogge, W. F. (2006). Source apportionment of molecular markers and organic aerosol. 2. Biomass smoke. *Environ. Sci. Technol.*, 40, 7811-7819.

Robinson, A. L., Donahue, N. M., Shrivastava, M. K., Weitkamp, E. A., Sage, A. M., Grieshop, A. P., Lane, T. E., Pierce, J. R., Pandis, S. N. (2007). Rethinking organic aerosols: Semivolatile emissions and photochemical aging. *Science,* 315, 1259-1262.

Rogge, W. F., Hildemann, L. M., Mazurek, M. A., Cass, G. R., Simoneit, B. R. T. (1991). Sources of fine organic aerosol. 1. Charbroilers and meat cooking operations. *Environ. Sci. Technol.*, 25, 1112-1125.

Rogge, W. F., Hildemann, L. M., Mazurek, M. A., Cass, G. R., Simoneit, B. R. T. (1993). Sources of fine organic aerosol. 2. Noncatalyst and catalyst-equipped automobiles and heavy-duty diesel trucks. *Environ. Sci. Technol.*, 27, 636-651.

Saxena, P., Hildemann L. M. (1996). Water-organics in atmospheric particles: A critical review of the literature and application of thermodynamics to identify candidate compounds. *J. Atmos. Chem.* 24, 57-109.

Schauer, J. J., Rogge, W. F., Hildemann, L. M., Mazurek, M. A., Cass, G. R., Simoneit, B. R. T. (1996). Source apportionment of airborne particulate matter using organic compounds as tracers. *Atmos. Environ.* 30, 3837-3855.

Schauer, J. J., Cass, G. R. (2000). Source apportionment of wintertime gas-phase and particle-phase air pollutants using organic compounds as tracers. *Environ. Sci. Technol.* 34, 1821-1832.

Schauer, J. J., Fraser, M. P., Cass, G. R., Simoneit, B. R. T. (2002). Source reconciliation of atmospheric gas-phase and particle-phase pollutants during a severe photochemical smog episode. *Environ. Sci. Technol.*, 36, 3806-3814.

Schulz, H., Harder, V., Ibald-Mulli, A., Khandoga, A., Koenig, W., Krombach, F., Radykewicz, R., Stampfl, A., Thorand, B., Peters, A. (2005). Cardiovascular effects of fine and ultrafine particles. *J. Aerosol Med.*, 18, 1-22.

Seinfeld, J. H., Erdakos, G. B., Asher, W. E., Pankow, J. F. (2001). Modelling the formation of secondary organic aerosol (SOA), 2. The predicted effects of relative humidity on aerosol formation in the alpha-pinene/, beta-pinene/, sabinene/, delta 3-carene/, and cyclohexane/ozone systems. *Environ. Sci. Technol.*, 35, 1806-1817.

Seinfeld, J. H., Pandis, S. N. (1998). Atmospheric Chemistry and Physics: From Air Pollution to Climate Change, John Wiley and Sons, New York.

Seinfeld, J. H., Pandis, S. N. (2006). Atmospheric chemistry and physics from air pollution to climate change. John Wiley, Sons, Inc., New York.

Shah, A. S. V., Langrish, J. P., Nair, H., McAllister, D. A., Hunter, A. L., Donaldson, K. (2013). Global association of air pollution and heart failure: a systematic review and meta-analysis. *The Lancet*, 382, 1039-1048.

Sheesley, R. J., Schauer, J. J., Zheng, M., Wang, B. (2007). Sensitivity of molecular marker-based CMB models to biomass burning source profiles. *Atmos. Environ.*, 41, 9050-9063.

Shen, Z. X., Cao, J. J., Arimoto, R., Han, Z. W., Zhang, R. J., Han, Y. M., Liu, S. X., Okuda, T., Nakao, S., Tanaka, S. (2009). Ionic composition of TSP and $PM_{2.5}$ during dust storms and air pollution episodes at Xi'an, China. *Atmos. Environ.*, 43, 2911-2918.

Shon, Z. H., Ghosh, S., Kim, K. H., Song, S. K., Jung, K., Kim, N. J. (2013). Analysis of water-soluble ions and their precursor gases over diurnal cycle. *Atmos. Res.*, 132-133, 309-321.

Simoneit, B. R. T., Schauer, J. J., Nolte, C. G., Oros, D. R., Elias, V. O., Fraser, M. P., Rogge, W. F., Cass, G. R. (1999). Levoglucosan, a tracer for cellulose in biomass burning and atmospheric particles. *Atmos. Environ.*, 33, 173-182.

Stone, E. A., Snyder, D. C., Sheesley, R. J., Sullivan, A., Weber, R., Schauer, J. J. (2008). Source apportionment of fine organic aerosol in Mexico City during the MILAGRO experiment 2006. *Atmos. Chem. Phys.*, 8, 1249-1259.

Strader, R., Lurmann, F., Pandis, S. (1999). Evaluation of secondary organic aerosol formation in winter. *Atmos. Environ.*, 33, 4849-4863.

Tan, J. H., Duan, J. C., Chen, D. H.,Wang, X. H., Guo, S. J., Bi, X. H., Sheng, G. Y., He, K. B., Fu, J. M. (2009). Chemical characteristics of haze during summer and winter in Guangzhou. *Atmos. Res.*, 94, 238-245.

Tao, J., Gao, J., Zhang, L., Zhang, R., Che, H., Zhang, Z., Lin, Z., Jing, J., Cao, J., Hsu, S.-C. (2014). $PM_{2.5}$ pollution in a megacity of southwest China: source apportionment and implication. *Atmos. Chem. Phys.*, 14, 8679-8699.

Tiwari, S., Srivastava, A. K., Chate, D. M., Safai, P. D., Bisht, D. S., Srivastava, M. K., Beig, G., (2014). Impacts of the high loadings of primary and secondary aerosols on light extinction at Delhi during wintertime. *Atmos. Environ.*, 92, 60-68.

Turpin, B., Huntzicker, J. (1995). Identification of secondary organic aerosol episodes and quantitation of primary and secondary organic aerosol concentrations during SCAQS. *Atmos. Environ.*, 29, 3527-3544.

Turpin, B. J., Saxena, P., Andrews, E. (2000). Measuring and simulating particulate organics in the atmosphere: Problems and prospects. *Atmos. Environ.*, 34, 2983- 3013.

Turpin, B. J., Lim, H. J. (2001). Species contributions to $PM_{2.5}$ mass concentrations: revisiting common assumptions for estimating organic mass. *Aerosol Sci. Tech.*, 35, 602-610.

Verma, S. K., Deb, M. K., Suzuki, Y., Tsai, Y. I. (2010). Ion chemistry and source identification of coarse and fine aerosols in an urban area of eastern central India. *Atmos. Res.*, 95, 65-76.

Wang, G. H., Huang, L. M., Gao, S. X., Gao, S. T., Wang, L. C. (2002). Characterization of water-soluble species of $PM_{10}$ and $PM_{2.5}$ aerosols in urban area in Nanjing, China. *Atmos. Environ.*, 36, 1299-1307.

Wang, Y., Zhuang, G., Tang, A., Yuan, H., Sun, Y., Chen, S., Zheng, A. (2005). The ion chemistry and the source of $PM_{2.5}$ aerosol in Beijing. *Atmos. Environ.* 39, 3771-3784.

Wang, Y., Zhuang, G. S., Zhang, X. Y., Huang, K., Xu, C., Tang, A., Chen, J. M., An, Z. S. (2006). The ion chemistry, seasonal cycle and sources of $PM_{2.5}$ and TSP aerosol in Shanghai. *Atmos. Environ.* 40, 2935-2952.

Watson, J. G. (1984). Overview of receptor model principles. *J. Air Pollut. Control Assoc.*, 34 (6), 619-623.

Watson, J. G., Robinson, N. F., Lewis, C. W., Coulter, C. T., Chow, J. C., Fujita, E. M., Conner, T. L., and Pace, T. G. (1998). CMB8 applications and validation protocol for PM2.5 and VOCs, prepared for U.S. Environmental Protection Agency, Research Triangle Park, NC by Desert Research Institute, Reno, NV.

Watson, J. G., Chow, J. C., Lowenthal, D. H., Stolzenburg, M. R., Kreisberg, N. M., Hering, S.V. (2002). Particle Size Relationships at the Fresno Supersite. *J. Air Waste Manage. Assoc.* 52, 822-827.

World Health Organization (WHO). (2013). Health effects of particulate matter. Policy implications for countries in eastern Europe, Caucasus and central Asia. Copenhagen: WHO Regional Office for Europe.

Xiao, S., Wang, Q. Y., Cao, J. J., Huang, R. J., Chen, W. D., Han, Y. M., Xu, H. M., Liu, S. X., Zhou, Y. Q., Wang, P., Zhang, J. Q., Zhan, C. L. (2014). Long-term trends in visibility and impacts of aerosol composition on visibility impairment in Baoji, China. *Atmos. Res.*, 149, 88-95.

Xing, Z. Y., Deng, J. J., Mu, C., Wang, Y., Du, K. (2014). Seasonal variation of mass absorption efficiency of elemental carbon in the four major emission areas in China. *Aerosol Air Qual. Res.*, 14, 1897-1905.

Yang, H. H., Cheng, S. K., Hsieh, L. T. (2004). Characterization of nitrate particulate dry deposition by vacuum-deposited thin film reaction method. *Atmos. Environ.,* 38, 1785-1793.

Yao, X. H., Chak, K. C., Fang, M., Cadle, S., Chan, T., Mulawa, P., He, K. B., Ye, B. M. (2002). The water-soluble ionic composition of $PM_{2.5}$ in Shanghai and Beijing. China. *Atmos. Environ.*, 36, 4223-4234.

Yin, L. Q., Niu, Z. C., Chen, X. Q., Chen, J. S., Zhang, F. W., Xu, L. L. (2014). Characteristics of water-soluble inorganic ions in $PM_{2.5}$ and $PM_{2.5-10}$ in the coastal urban agglomeration along the Western Taiwan Strait Region, China. *Environ. Sci. Pollut. Res.*, 21, 5141-5156.

Zhao Y. L., Gao Y. (2008). Mass size distributions of water-soluble inorganic and organic ions in size-segregated aerosols over metropolitan Newark in the US east coast. *Atmos. Environ.*, 42, 4063-4078.

Zhang, R., Jing, J., Tao, J., Hsu, S.-C., Wang, G., Cao, J., Lee, C. S. L., Zhu, L., Chen, Z., Zhao, Y., Shen, Z. (2013). Chemical characterizations and source apportionment of $PM_{2.5}$ in Beijing: Seasonal perspective. *Atmos. Chem. Phys.*, 13, 7053-7074.

Zhang, T., Cao, J. J., Tie, X. X., Shen, Z. X., Liu, S. X., Ding, H., Han, Y. M., Wang, G. H., Ho, K. F., Qiang, J. (2011). Water-soluble ions in atmospheric aerosols measured in Xi'an, China: seasonal variations and sources. *Atmos. Res.*, 102, 110-119.

Zhang, Y, Schauer, J. J., Zhang, Y., Zeng, L., Wei, Y., Liu, Y. (2008). Characteristics of Particulate Carbon Emissions from Real-World Chinese Coal Combustion. *Environ. Sci. Technol.*, 42, 5068-5073.

Zheng, M., Cass, G. R., Schauer, J. J., Edgerton, E. S. (2002). Source Apportionment of $PM_{2.5}$ in the Southeastern United States Using Solvent-Extractable Organic Compounds as Tracers. *Environ. Sci. Technol.*, 36: 2361-2371.

Zheng, M., Salmon, L. G., Schauer, J. J., Zeng, L. M., Kiang, C. S., Zhang, Y. H., Cass, G. R. (2005). Seasonal Trends in $PM_{2.5}$ Source Contributions in Beijing, China. *Atmos. Environ.*, 39, 3967-3976.

Zheng, M., Ke, L., Wang, F., Cass, G. R., Schauer, J. J., Edgerton, E. S., Russell, A. G. (2007). Source apportionment of daily $PM_{2.5}$ at Jefferson Street, Atlanta, GA during summer and winter. *J. Air Waste Manage. Assoc.*, 57, 228-242.

Zhou, J. B., Xing, Z. Y., Deng, J. J., Du, K. (2016). Characterizing and sourcing ambient $PM_{2.5}$ over key emission regions in China I: Water-soluble ions and carbonaceous fractions. *Atmos. Environ.*, 135, 20-30.

Zhou, S. Z., Wang, Z., Gao, R., Xue, L. K., Yuan, C., Wang, T., Gao, X. M., Wang, X. F., Nie, W., Xu, Z., Zhang, Q. Z., Wang, W. X. (2012). Formation of secondary organic carbon and long-range transport of carbonaceous aerosols at Mount Heng in South China. *Atmos. Environ.*, 63, 203-212.